Title
Synthesis of Yttrium and Aluminum Complexes Supported by a Mono-Substituted Ferrocene Ligand

Author
Gao, Jun

Publication Date
2015

Peer reviewed|Thesis/dissertation

UNIVERISTY OF CALIFORNIA

Los Angeles

Synthesis of Yttrium and Aluminum Complexes Supported by a Mono-Substituted Ferrocene Ligand

A thesis submitted in partial satisfaction

of the requirements for the degree Master of Science

in Chemistry

by

Jun Gao

2015

ABSTRACT OF THE THESIS

Synthesis of Yttrium and Aluminum Complexes Supported

by a Mono-Substituted Ferrocene Ligand

by

Jun Gao

Master of Science in Chemistry

University of California, Los Angeles, 2015

Professor Paula Loredana Diaconescu, Chair

Ferrocene chelating ligands provide good stability of the resulting metal complexes and redox-switchable control in chemical processes catalyzed by those complexes. In comparison to traditional di-substituted ferrocene tetradentate ligands, mono-substituted tridentate ferrocene ligands may form metal complexes with a more open coordination sphere around the metal center that may allow an increased preference for substrate coordination. In addition, a mono-substituted ferrocene ligand allows the investigation of the through bond influence of the ferrocenyl group on catalytic metal centers by increasing the metal-iron distance. In this thesis, the design, synthesis, and characterization by ^{1}H NMR spectroscopy of a novel mono-substituted ferrocene ligand are described. To explore its ability to support metal complexes with high activity and redox-

switchable in polymerization reactions, yttrium alkoxide and aluminum alkyl complexes were also synthesized and characterized by ^{1}H NMR spectroscopy.

The thesis of Jun Gao is approved.

Alexander Michael Spokoyny

Ohyun Kwon

Paula Loredana Diaconescu, Committee Chair

University of California, Los Angeles

2015

DEDICATION

This work is dedicated to my mother for her endless support.

TABLE OF CONTENTS

TABLE OF FIGURES

NOMENCLATURE

δ	Chemical shift
BBL	β-butyrolactone
CL	ε-caprolactone
Cp	cyclopentadienyl
Et_2O	diethyl ether
Fc	mono-substituted ferrocenyl
fc	1,1' -disubstituted ferrocenediyl
$FeCp_2$	ferrocene
$^{n}BuLi$	*n*-butyllithium
DCM	dichloromethane
DFT	Density functional theory
HOMO	Highest occupied molecular orbital
NMR	Nuclear magnetic resonance
TBE	1,1,2,2-tetrabromoethane
THF	tetrahydrofuran
TMEDA	N,N,N',N'-tetramethylethylenediamine

ACKNOWLEDGEMENTS

I would like to express my sincere gratitude to my advisor Professor Paula Loredana Diaconescu for her continuous support of my studies and related research, and for her patience, motivation, and immense knowledge.

I would also like to thank the other group members, Stephanie Quan, Mark Abubekerov, Jon Brosmer, and Dr. Xinke Wang, for their insightful comments and encouragement.

Chapter 1: Introduction

Organic derivatives of metals form when organic fragments associate with metal centers. Among these compounds are organometallic compounds that contain at least one direct metal-carbon bond or include a bond between an organic carbon and an atom that is less electronegative than carbon[1,2]; such compounds are widely used in homogeneous catalysis. Although organometallic compounds of iron have played a lesser role than precious metals in homogeneous catalysis, ferrocene is one of the most recognized compounds by chemists as an organotransition metal molecule[3].

1.1 FERROCENE

Ferrocene is the first known metallocene and was discovered in the early 1950s[4]. Since its discovery, this sandwich-structured compound has attracted a lot of attention and intensive studies have been conducted. Pioneering researchers initially investigated the basic properties and reactivity of ferrocene. Numerous applications were developed following the investigation of this compound's properties.

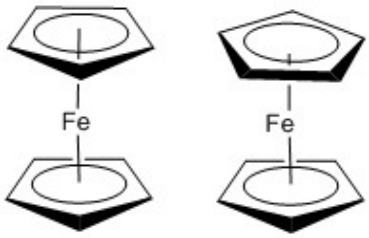

Figure 1-1: The structure of ferrocene in which the Cp rings can rotate freely.

Ferrocene is diamagnetic and stable. It possess several structural orientations as the two cyclopentadienyl rings can rotate[5] (Figure 1-1). Having a metal center hindered by surrounding Cp rings, its molecular and electrochemical properties give ferrocene an easily accessible one-electron Nernstian couple with a medium-independent redox potential[6]. This property makes ferrocene a suitable candidate as a redox standard[7]. One of the most important properties of ferrocene is its ability to undergo a reversible redox reaction which allows it to switch back and forth between ferrocene and the ferrocenium cation[8] (Figure 1-2). When oxidized, removal of a bonding electron led to longer Fe-C bond lengths, thus the distance between iron and the Cp ring increases, making ferrocenenium slightly larger than ferrocence[9].

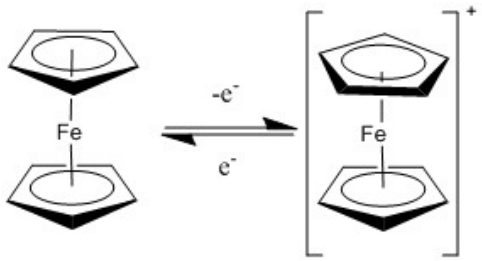

Figure 1-2: The ferrocene/ferrocenium redox pair.

1.2 Ferrocene in Materials and Biomolecules

Applications of ferrocene derivatives can be found in numerous areas such as catalysis, materials science, and biomedicinal chemistry[10]. Ferrocene can assist in the building of nano-structures such as nanospheres[11] and nanotubes[12]. Ferrocene derivatives can also

modify carbon nanofibers to provide a synthetic approach toward high-surface-area electrodes with high stability and electrochemical properties[13]. Materials with monolayer and multilayer ferrocene-containing films whose thicknesses are controlled by molecular concentrations and reaction times have also been developed[14]. Ferrocene either covalently bound to a polymer or trapped within a polymer matrix, also has a fundamental study value and practical applications[15]. Ferrocene containing compounds and polymers also have applications in molecular recognition and sensing systems[16].

The geometry of ferrocene allows rotary motions at the molecular level, one of the most common mechanical processes in molecular level energy conversion. Utilizing the rotation of Cp rings linked to the iron center, ferrocene rotors have been achieved through chemical methods, such as (de)-protonation[17], photo-operated systems[18], and redox triggers[19].

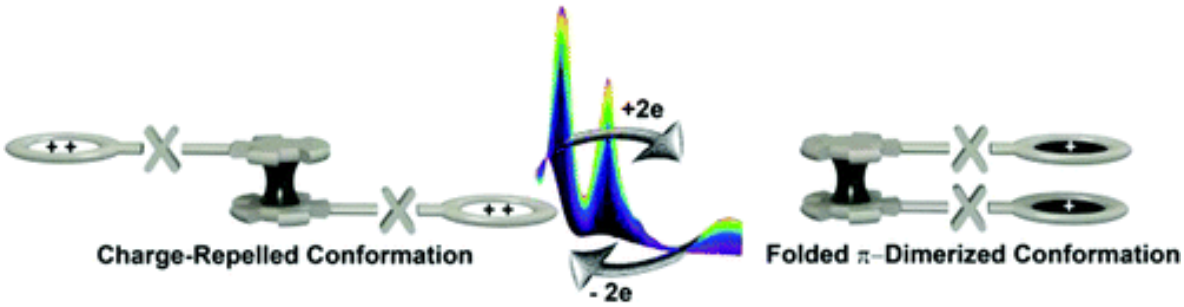

Figure 1-3: A molecular carousel triggered by electron transfer in which the Cp rings are substituted with π-dimerizable bipyridinium groups. The repulsive charges and maximum overlap of HOMO in each configuration are the driving forces for the rotation. Reprinted with permission[20].

Ferrocene and its derivatives are also popular molecules for biological applications because of their stability in aqueous and aerobic environments, accessibility of various derivatives,

and electrochemical properties[21]. They can function as labels by covalently bonding to biomolecules such as peptides[21] and nucleic acids[22]. They can induce biological activities such as plant growth regulation[23] and anti-bacterial and anti-fungal activities[24]. Ferrocene containing compounds are also frequently used in medicine such as anti-cancer, anti-malarial, and anti-HIV drugs[25].

1.3 Ferrocene-based Ligands in Coordination Chemistry

Ferrocene derivatives are widely investigated as organometallic scaffolds. Ferrocene can undergo electrophilic aromatic substitutions much easier then common aromatic compounds due to the negative charge of the Cp rings[26]. Heteroatoms including nitrogen, oxygen, phosphorus, and boron are the most encountered substitutions linked to the ferrocenyl group, while carbon atoms involving a π-system[27,28] are also frequently observed. The common pathways of derivatizing ferrocene are shown in Figure 1-4. Although ferrocene is air stable, the presence of substitution may interfere with its aromatic system and lead to decreased stability and decomposition in air. Thus many ferrocene-based ligands are handled under inert atmosphere. Some ferrocene derivatives are widely used and investigated as homogeneous catalysts.

1.3.1 Geometrical Considerations

As a large family of ligands in homogeneous catalysis[30], one significant function of ferrocene derivatives is their enantioselectivity. The sandwich-structure of ferrocenyl

derivatives empowers their capability of tuning chirality around a catalytic center[31]. When a bulk ferrocenyl ligand is oriented with a particular configuration around a metal center, the geometry of the product can be predetermined. The asymmetric enantiometric 1,2-heterodisubstituted ferrocenes, which produce planar chirality (Figure 1-5), have been intensively studied[32] for this purpose.

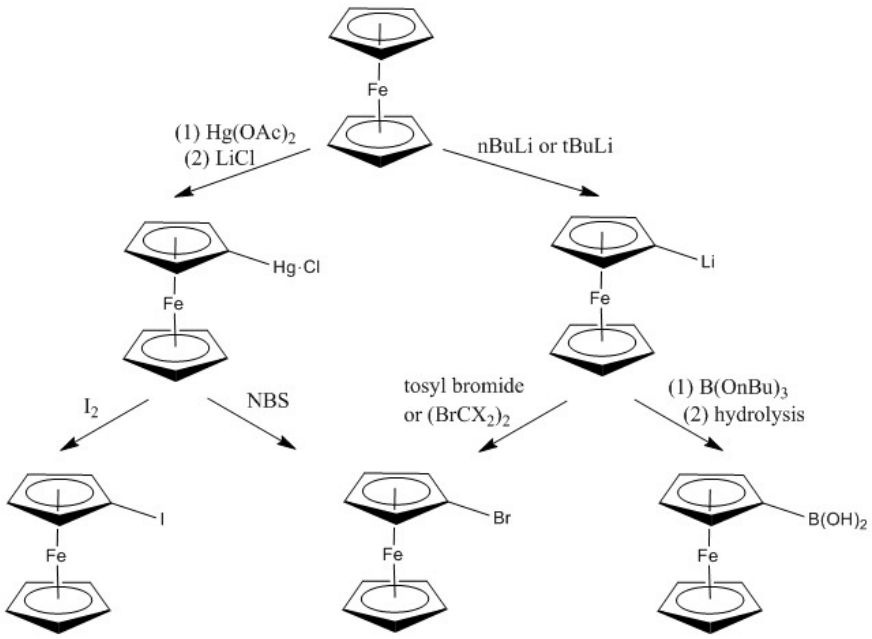

Figure 1-4: Common methods of synthesizing ferrocenyl derivatives. Reprinted with permission[29].

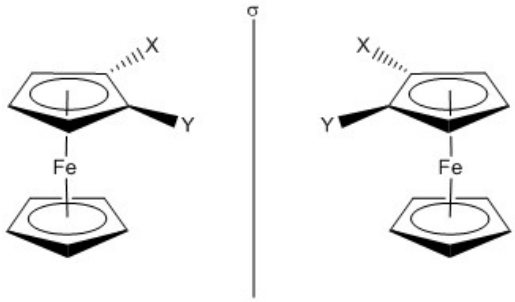

Figure 1-5: Enantiomeric heterodisubstituted ferrocenes and the planar chirality results from the structure. Reprinted with permission[32].

In 1996, Wang and coworkers introduced ferrocene into a 1,3-dicarbonyl compound to produce an asymmetry-inducing chiral ligand (Figure 1-6). This design was based on the C_2 symmetry of the ligand and the chirality provided by the ferrocenyl group. With experimental trials on various asymmetric catalytic reactions, metal complexes supported by this ligand gave notable selectivity and efficiency in the silylcyanation of benzaldehyde[33].

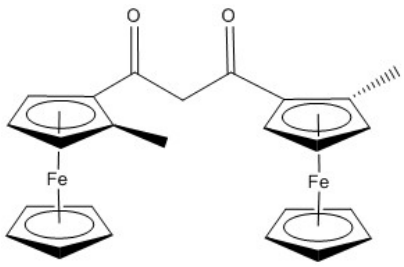

Figure 1-6: (R,R)-1,3-bis(2-methylferrocenyl)propane-1,3-dione. A ferrocene containing chiral ligand that supports metal complexes catalyze asymmetric silylcyanation of benzaldehyde efficiently. Reprinted with permission[33].

One well-known example of enantioselective reactions that are carried out by planar-chiral ferrocene-based ligands is Josiphos-catalyzed asymmetric homodimerization of ketoketenes (Figure 1-7). This reaction demonstrates a high selectivity of up to 96% *ee* while maintaining decent yields. In addition, complexes supported by Josiphos ligands also possesses diastereoselectivity in ring-opening reactions of enantioenriched ketoketene dimers[34].

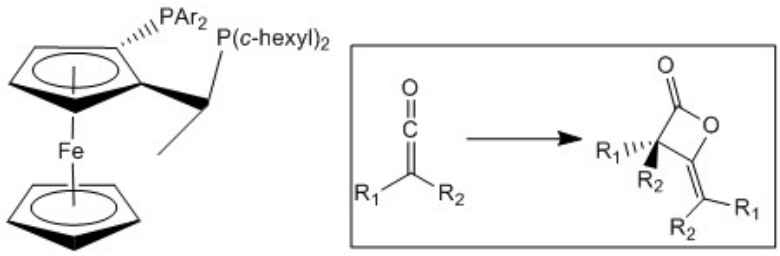

Figure 1-7: Asymmetric homodimerization of ketoketenes catalyzed by complexes supported by Josiphos ligands. Reprinted with permission[34].

Enantioselective catalyzed processes are not exclusively used in the laboratory, but also have numerous applications within industry. The process catalyzed by iridium complexes supported by Xyliphos ligands affords the largest known scale of imine hydrogenation (Figure 1-8). Every year, the amine product from this reaction is enough to produce more than 10,000 tons of the herbicide (S)-metolachlor[20].

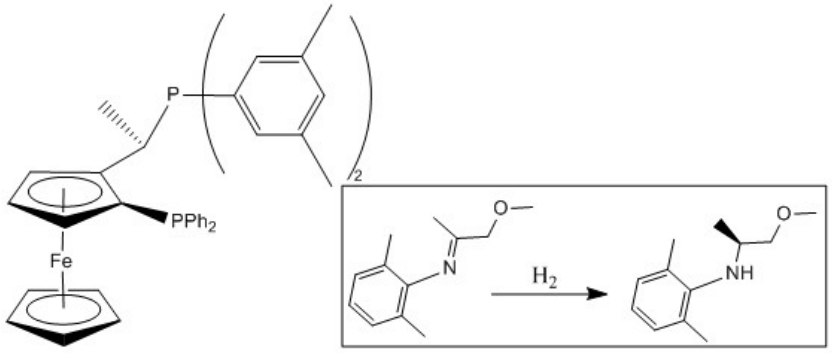

Figure 1-8: Enantioselective imine hydrogenation catalyzed by complexes supported by a xyliphos ligand. The reaction is on an industrial scale with high selectivity and turnover frequency. Reprinted with permission[20].

1.3.2 Electronic Considerations

Another powerful function of ferrocene-based ligands is the possible electron tunability at metal center which is a result of the rapid and reversible redox reaction involving the iron atom in ferrocene[31]. This property enables synergistic effects in complexes supported by ligands containing ferrocene scaffolds and results in enhanced catalytic activities in a variety of types of reactions such as olefin[35] and ring-opening[36] polymerization. For example, our group has synthesized an indium complex supported by a salfen ligand containing a ferrocene scaffold which gives the highest reported activity toward ε-caprolactone (CL) and β-butyrolactone (BBL) polymerization (Figure 1-9).

The crucial role of the ferrocene backbone in metal complexes used in catalysis has been previously investigated by our group. A study on a series of mono(1,1′-diamidoferrocene) uranium complexes utilizing spectroscopic techniques and computational methods revealed that the reduction potentials of uranium are significantly higher than those of the uranium complexes supported by pentamethylcyclopentadienyl ligands. This suggests that ferrocene diamides are significantly stronger electron donors[37].

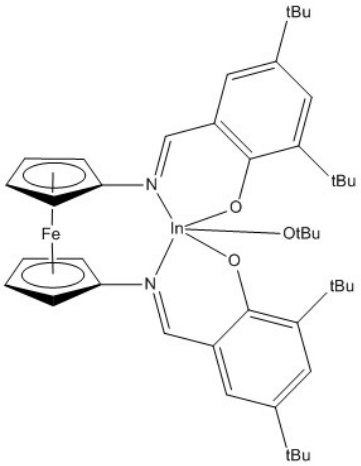

Entry	Monomer	[Monomer]/[Cat]	Solvent	Time (min)	% Conversion (temp)
1	BBL	100	Toluene	30	99
2	BBL	200	Toluene	45	99
3	BBL	300	Toluene	45	99
4	BBL	400	Toluene	60	99
5	CL	500	Toluene	2	99
6	CL	2000	Toluene	30	99

Figure 1-9: An indium complex supported by a ferrocene-based ligand and data showing high conversion and monomer to catalyst ratio for the ring-opening polymerization of CL and BBL.

One mechanism of ferrocene-based ligands influencing the reactivity of a catalytic metal center is the direct metal-iron interaction (Figure 1-10). The electrophilicity of a metal center changes when its chemical environment[38,39] or oxidation state[40] changes. Experiments have revealed that when the electrophilicity changes, the distance between the iron center of the ferrocence backbone and the metal center of a complex supported by the ferrocene-based ligand varies. This observation suggests a weak donor-acceptor type of bond between the electron-rich iron and the electropositive metal ion. When they are in a close proximity, the iron center acts as a Lewis base that stabilizes the Lewis acidic metal center in the corresponding complex[41–43].

The communication between iron in ferrocene and another metal can also occur through bonds between the Cp ring and the metal center. The degree of conjugation affects the redox properties of a ferrocenyl ligand containing complex. Westwood and coworkers

showed that when a ferrocene backbone is at the vinyl position of a conjugated π-electron system, a through-bond communication is permited[44]. Moreover, a longer conjugated link has been demonstrated to weaken the through-bond effects[45]. If a complex already contains a redox-active metal center, the addition of ferrocenyl units may increase the reactivity of the complex compared to an analogous complex without a redox-active iron[46].

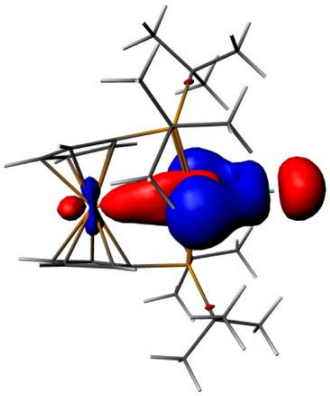

Figure 1-10: Molecular orbitals of metal-metal interaction between iron center of ferrocene backbone and the catalytic center. Reprinted with permission[41].

Notably, not only can the ferrocene unit affect a metal center, but the redox potential of the ferrocene backbone can also be influenced by other moieties in a complex. The electron-withdrawing nature of a metal center makes iron more difficult to oxidize. In addition, the redox potential of the ferrocene unit also strongly depends on the substitution of the Cp ring[47] and the ligand environment of the metal center[44,48].

1.3.3 Redox Considerations

Ferrocene-based ligands are especially useful when supporting redox-switchable catalysts. The iron center can change its oxidation state reversibly between the reduced ferrocene and oxidized ferrocenium states by simple chemical methods. When such a conversion occurs, a metal complex supported by the corresponding ferrocene ligand may have distinct reactivity toward different substrates depending on the ferrocene's oxidation state. By triggering the redox reaction of a ferrocene backbone, the catalytic activity of a compound is effectively switched on or off, thus enabling a desirable selectivity in processes catalyzed by the complex of interest.

An early utilization of the redox-switch property of ferrocene was a phase tag developed by Plenio and coworkers[49] (Figure 1-11). The ferrocene component enables a redox-switchable phase tag, which changes the solubility of the ferrocene containing complex upon oxidation or reduction. When such a complex is used in a catalytic process, it can be conveniently separated from the reaction mixture and recycled by precipitation.

The ability of turning on and off the catalytic activity of a compound provides a basis for controlled catalyzed processes. While redox control can also be accomplished by changing the oxidation state of a catalytic metal center[50], the involvement of a ferrocene backbone allows the use of a wider range of strong Lewis acidic metals, thus affording, in principle, a larger number of catalyzed reactions.

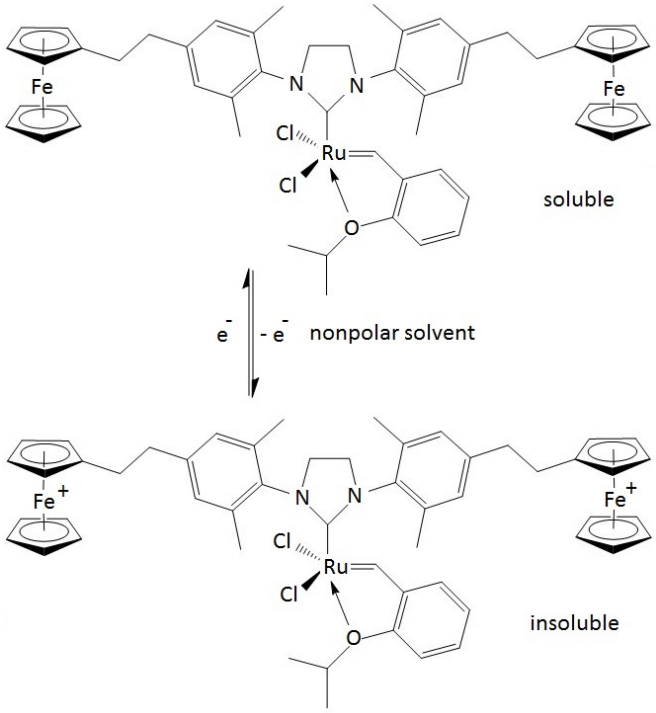

Figure 1-11: Ferrocenyl phase tag developed by Plenio and coworkers. The redox-switch controls solubility of the complex and makes the separation and recycling of catalytic active species possible. Reprinted with permission [49].

Our group has synthesized a phosfen ligand (Figure 1-12), which allows redox control over the activities of the yttrium and indium complexes it supports[51]. When supported by a phosfen ligand, complexes with different metal centers give different catalytic activities toward the ring-opening polymerization of trimethylene carbonate. The activity of the indium complex is switched off when the ferrocene backbone is in its oxidized form, whereas the yttrium complex is switched on under the same conditions. Following the investigation on redox-switches that simply turn reactivity on and off, other ferrocene-based ligands were also developed for the purpose of achieving a one-pot copolymerization reaction (Figure 1-13). Some metal complexes supported by salfan and thiolfan ligands

synthesized by our group represent an approach toward this goal. When switching between the ferrocene and ferrocenium states using redox reagents, the reactivity of a metal complex toward L-lactide and ε-caprolactone is altered. The change in reactivity leads to a difference in reaction rates, and therefore results in block copolymers formed by these monomers[36].

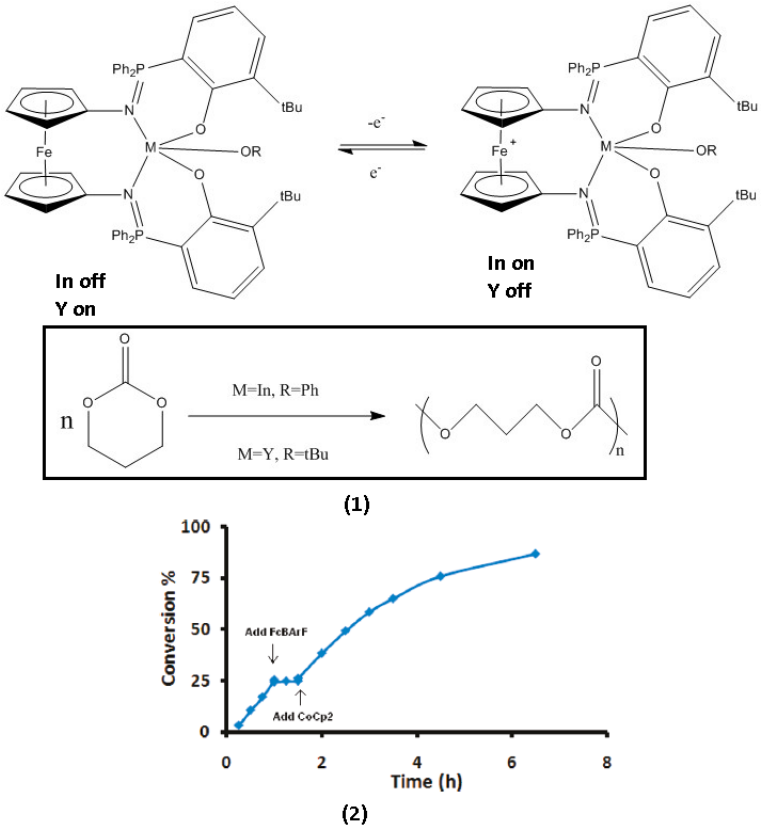

Figure 1-12: (1) Indium and yttrium complexes supported by a phosfen ligand whose catalytic activities are chemically controlled. (2)The conversion plot demonstrates reactivity of the yttrium complex toward L-lactide polymerization when it is switched back and forth between reduced and oxidized forms. Reprinted with permission[51].

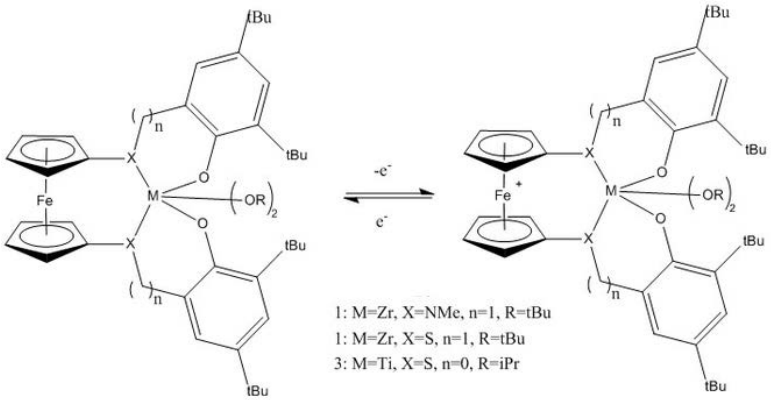

initiator	monomer	time (h)	conversion (%)	M_n GPC	M_n calcd	PDI
1^{red}	LA	2	90	7.31	6.77	1.16
1^{ox}	LA	2	<5			
2^{red}	LA	8	93	7.83	6.70	1.10
2^{ox}	LA	8	<5			
3^{red}	LA	60	82	4.49	5.90	1.14
3^{ox}	LA	36	<5			
1^{red}	CL	24	<5			
1^{ox}	CL	24	98	6.95	5.59	1.06
2^{red}	CL	1.5	57	3.87	3.25	1.10
2^{ox}	CL	1.5	92	8.26	5.24	1.14
3^{red}	CL	2	<5			
3^{ox}	CL	4	48	3.20	2.70	1.12

Figure 1-13: Complexes of group 4 metals supported by thiolfan and salfan ligands and experimental results of their reactiviy toward polymerization with L-lactide and ε-caprolactone monomers. Reprinted with permission[36].

Ferrocene's geometric, electronic, and redox properties makes the metal complexes supported by such scaffolds useful in many fields[52]. Following the synthesis and investigation of existing ferrocene ligands and the complexes supported by them, new questions arise: What parameters of a ferrocene-based ligand determine the properties of the resulting complexes and how can we design more reactive and selective compounds to be used in catalysis. Herein is described the synthesis of a novel ferrocene-based ligand, as well as the corresponding yttrium and aluminum complexes.

Chapter 2: A Mono-Substituted Ferrocene Ligand

2.1 INTRODUCTION

Due to the outstanding behavior in supporting a wide range of reactivity for the resulting metal complexes, our group focused on ferrocene-based chelating ligands. The ability of enforcing an open space on one side of a metal center for substrate coordination, stabilizing a metal center, and triggering a redox-switch makes them desirable ancillary ligands. Pursuing a deeper understanding of how substituents influence the properties of a ligand, we have conducted systematic studies on several types of ferrocene-based ligands, as well as designed and synthesized new ligands.

Ferrocene Schiff base ligands provide a class of widely used chelating ligands[53]. Our group inspected two types of complexes supported by this class of ligands where the ligands are based on imine and iminophosphrane groups (Figure 2-1). Salfen ligands, which are based on imine linkers, provide high reactivity for the complexes they support, including an indium complex with the highest reported activity toward CL and BBL polymerization (Figure 1-9), and a rare example of a cerium(IV) alkoxide catalyst for lactide polymerization[54]. Phosfen ligands, which are based on iminophosphrane groups, have demonstrated the ability to support redox-switchable type of complexes[51]. A combined study of cerium complexes supported by these two series of ligands revealed that the iminophosphorane group makes a ligand more easily oxidized than the imine group and that cerium(IV) is not involved in the redox behavior of ligands[55].

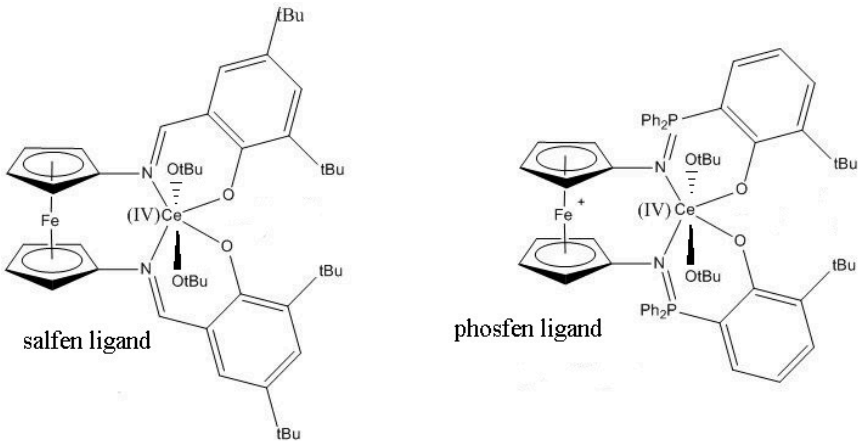

Figure 2-1: Two series of Schiff base metal complexes where each series was supported by a ferrocene-based ligand incorporating imine or iminophosphorane groups as different N = X functionalities. Reprinted with permission[55].

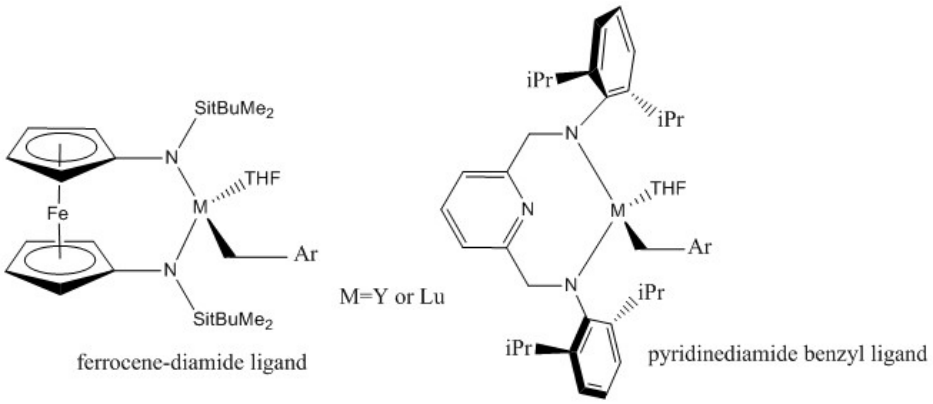

Figure 2-2: Group 3 metal complexes supported by ferrocene-diamide and pyridinediamide benzyl ligands. Reprinted with permission[56].

Chelating ferrocene-diamides represent a versatile ligand framework. The electron donating amine groups on Cp rings enable easier oxidation of the ferrocene backbone by increasing electron density of the iron center. When incorporating different substituents, including alkyl, aryl, and silyl groups, aromatic substituents on the nitrogen atoms influence the electronic structure the most[57], although the oxidation potential of 1,1'-

ferrocene diamides do not vary significantly. To probe the influence of the ferrocenyl group on reactivity with aromatic N-heterocycles, a comparison between the ferrocene-based and the analogous pyridine diamide benzyl group 3 metal complexes was made[56] (Figure 2-2). The study showed that asimilar reaction with 1-methylimidazole, 2-picoline, and isoquinoline occurred, however, ferrocene-based complexes gave more types of reactions and a larger substrate scope than the pyridine diamide compounds.

Recently, nickel(II) and zinc(II) complexes supported by ferrocene-chelating heteroscorpionate were synthesized and characterized[58] (Figure 2-3). This design incorporates the stereoelectronic properties of poly(pyrazolyl)borates[59] and the redox activity of ferrocene into a new type of ligand. Besides, the tridentate ferrocene-based heteroscorpionate ligand coordinates less strongly to a metal than the ferrocene diamides, while providing a less crowded metal center and a weaker metal-iron interaction. Cyclic voltammetry and DFT calculation studies showed that the nickel complexes have a combination of reversible and irreversible redox processes from both nickel and iron metal centers, whereas the zinc complexes have only a single, iron based, reversible redox process due to the redox inactive nature of zinc.

Although 1,1'-disubstituted ferrocene-based ligands are widely used in many applications, the bulk around the active metal centers produced by the ligands may hinder the binding of substrates in catalysis. Under this consideration a mono-substituted ferrocene-based ligand is potentially capable of forming metal complexes with more open coordination spheres than ligands derived from 1,1’-disubstituted ferrocenes. Therefore a mono-

substituted tridentate ferrocene-based ligand was designed (Figure 2-4) and synthesized for additional investigations on how ferrocene-based ligands influence the activity of the metal complexes they support.

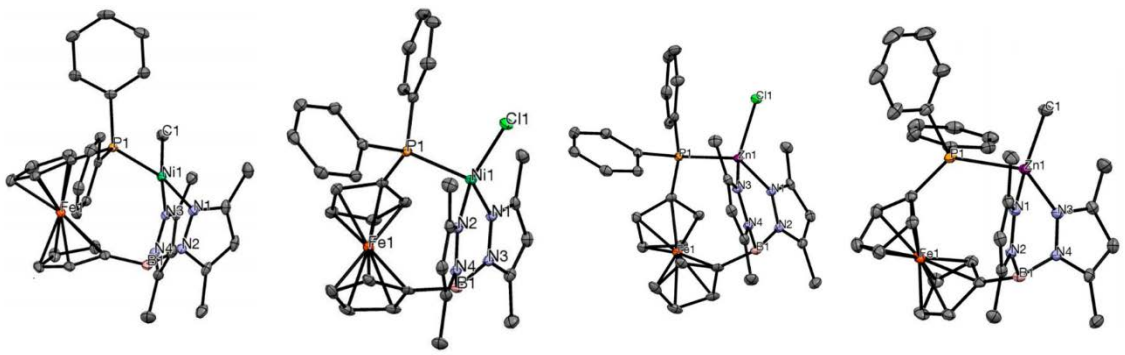

Figure 2-3: Molecular structure drawing of nickel and zinc complexes supported by a heteroscorpionate ligand with thermal ellipsoids at 50% probability. From left to right: ($fc^{P,B}$)NiMe, ($fc^{P,B}$)NiCl, ($fc^{P,B}$)ZnCl, ($fc^{P,B}$)ZnMe. Hydrogen and solvent atoms are omitted for clarity. Reprinted with permission[58].

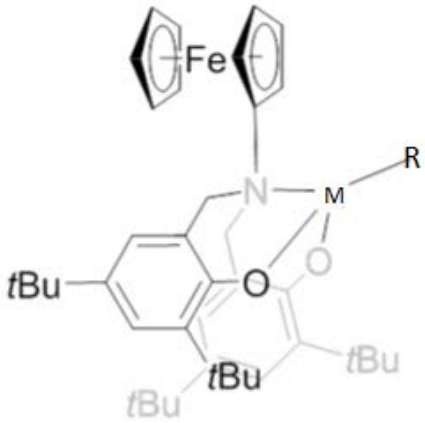

Figure 2-4: Structure of a metal complex supported by Fc^{ONO}.

2.2 EXPERIMENTAL

All reactions were performed using standard Schlenk techniques or in an MBraun drybox (less than 1 ppm of O_2/H_2O) unless noted otherwise. All glassware were stored in an oven at 425 K or higher before being brought into the drybox. Solvents were purified using a two-column solid-state purification system by the method of Grubbs[60] and transferred to the drybox without exposure to air. NMR solvents were obtained from Cambridge Isotope Laboratories, degassed, and stored over activated molecular sieves prior to use. NMR spectra were recorded at ambient temperature on Bruker AV-300. Proton chemical shifts are given relative to residual solvent peaks. All reagents were acquired from commercial sources and used as received unless otherwise noted.

2.2.1 Synthesis of aminoferrocene[61]

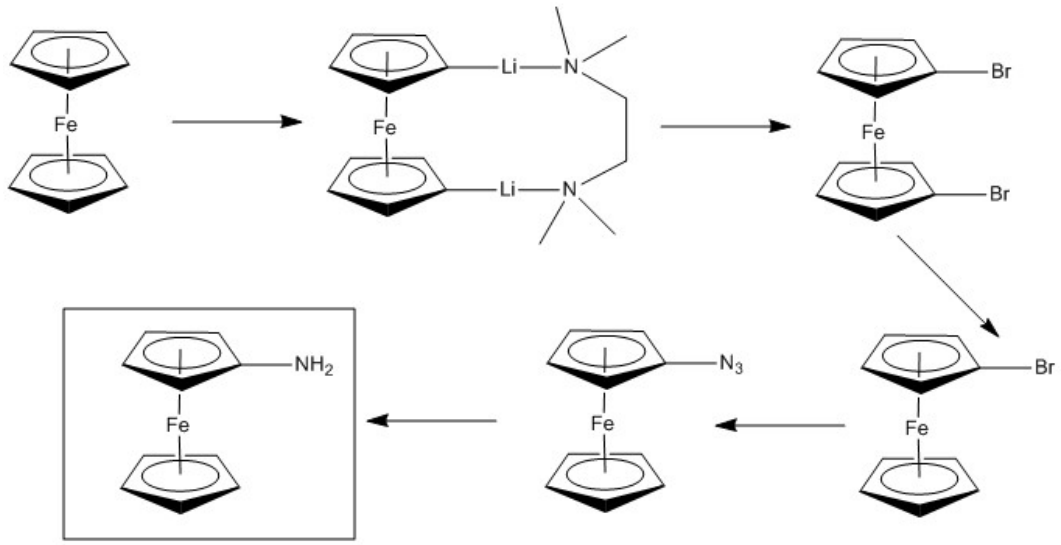

Figure 2-5: Scheme of aminoferrocene synthesis.

1,1'-dilithioferrocene[62]

To a stirring solution of ferrocene (6.910 g, 37.1 mmol) and TMEDA (5.175 g, 44.52 mmol) in hexanes (250 mL) ^{n}BuLi (2.0 M solution in hexanes, 39 mL, 78 mmol) was added dropwise over the course of half an hour. The reaction mixture was stirred for 12 h then filtered over a medium frit yielded product as an orange solid (9.0295 g, 77.6%).

1,1'-dibromoferrocene[61]

To a stirring solution of 1,1'-dilithioferrocene (9.0295 g, 28.8 mmol) in diethyl ether (50 mL) 1,1,2,2-tetrabromoethane (21.88 g, 63.3 mmol) was added dropwise at -78 °C over the course of half an hour. After stirring for 7 h the reaction mixture was warmed up to room temperature and was stirred for another 12 h. The reaction mixture was then opened to air and quenched with water (50 mL). The resulting biphasic system was filtered over Celite using a frit. The aqueous layer was extracted three times with diethyl ether (50 mL). The combined organic layer was washed with water (30 mL) and dried over anhydrous magnesium sulfate. The solvent was removed under reduced pressure to produce an oily brown crude product. The product was crystallized in methanol yielded the product as a brown solid (8.281g, 83.7%). ^{1}H NMR ($CDCl_3$, 300 MHz, ppm): δ 4.422 (t, J = 1.3 Hz, 2H, Cp - H), 4.167 (t, J = 1.3 Hz, 2H, Cp - H).

bromoferrocene[63]

To a stirring solution of 1,1'-dibromoferrocene (6.66 g, 19.4 mmol) in THF (20 mL) ^{n}BuLi (2.5 M solution in hexanes, 8.0 mL, 19.9 mmol) was added dropwise at -78 °C over the course of half an hour. The reaction mixture was stirred at -78 °C for 1 h, opened to air and

quenched with water (3 mL) dropwise at -78 °C, and then warmed up to room temperature over 1 h. Additional water (50 mL) was added and the mixture was stirred for 1 h. The volatile material was removed by reduced pressure. The residue was extracted three times with ethyl ether (50 mL). The combined organic layer was washed with saturated iron(III) chloride aqueous solution, dried over anhydrous magnesium sulfate. The solvent was removed under reduced pressure to produce an oily brown crude product. The product was crystallized in methanol yielded the product as a brown solid (3.120 g, 61.3%). ^{1}H NMR ($CDCl_3$, 300 MHz, ppm): δ 4.407 (t, *J* = 1.4 Hz, 2H, substituted Cp - H), 4.224 (s, 5H, unsubstituted Cp - H), 4.095 (t, *J* = 1.4 Hz, 2H, substituted Cp - H).

azidoferrocene[63]

To a stirring slurry of bromoferrocene (1.1089 g, 4.18 mmol) and CuCl (0.485 g, 4.90 mmol) in reagent alcohol (30 mL) an aqueous solution of NaN_3 (0.629 g, 9.67 mmol) in water (3 mL) was added in dark at room temperature in air and stirred for 20 h. The reaction mixture was quenched with water (30 mL) and stirred for half an hour, then filtered through Celite. The filtrate was extracted six times with hexanes (60 mL). The combined organic layer was dried over anhydrous magnesium sulfate. The solvent was removed under reduced pressure to produce an oily brown crude product. The product was crystallized in hexanes yielded the product as a dark brown solid (0.601 g, 63.2%). ^{1}H NMR (C_6D_6, 300 MHz, ppm): δ 4.015 (s, 5H, unsubstituted Cp - H), 3.994 (t, *J* = 1.9 Hz, 2H, substituted Cp - H), 3.663 (t, *J* = 1.9 Hz, 2H, substituted Cp - H).

aminoferrocene[61]

In a Schlenk tube azidoferrocene (692 mg, 3.05 mmol) was dissolved in methanol (20 mL) and Pd/C catalyst (34.6 mg) was charged. The reaction flask was covered with aluminum foil. Hydrogen gas was blown into the flask repeatedly over the course of 24 h in dark. The reaction mixture was filtered through Celite. The solvent was removed under reduced pressure to yield the product as an orange red solid (570 mg, 92.9%). ^{1}H NMR (C_6D_6, 300 MHz, ppm): δ 3.975 (s, 5H, unsubstituted Cp - H), 3.726 (t, J = 1.8 Hz, 2H, substituted Cp - H), 3.691 (t, J = 1.8 Hz, 2H, substituted Cp - H).

2.2.2 Synthesis of 6-bromomethyl-2,4-di-*tert*-butyl-phenol

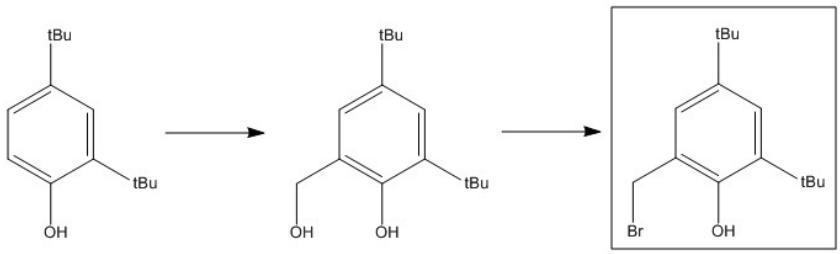

Figure 2-6: Scheme of 6-bromomethyl-2,4-di-tert-butyl-phenol synthesis.

6-methylhydroxyl-2,4-di-*tert*-butyl-phenol[64]

To a solution of 2,4-di-*tert*-butyl-phenol (20.61 g, 100 mmol) in 60 mL methanol sodium hydroxide (4.40 g, 110 mmol) was added in air. The mixture was stirred for an hour until NaOH was dissolved. Formaldehyde (36% aqueous solution, 30 mL, 384 mmol) was added. The reaction mixture was stirred for 26 h at room temperature and quenched with

water (300 mL). The solution was brought to a pH of 2-3 with 36% aqueous HCl solution and vigorous stirring. The mixture was extracted three times with dichloromethane (50 mL). The combined organic layer was dried over anhydrous magnesium sulfate. The solvent was removed under reduced pressure to produce a yellow oil. The crude product was crystallized in hexanes yielded the product as a white solid (17.878 g, 75.7%). ^{1}H NMR (C_6D_6, 300 MHz, ppm): δ 7.944 (s, 1H, Hydroxyl - H), 7.476 (d, *J* = 2.4 Hz, 1H, aryl - H), 6.705 (d, *J* = 2.4 Hz, 1H, aryl - H), 4.223 (d, *J* = 2.8 Hz, 2H, methyl - H), 1.654 (s, 9H, *tert*-butyl - H), 1.328 (s, 9H, *tert*-butyl - H).

6-bromomethyl-2,4-di-*tert*-butyl-phenol[65]

To a stirring solution of 6-methylhydroxyl-2,4-di-*tert*-butyl-phenol (12.822 g, 54.3 mmol) in chloroform (150 mL) PBr_3 (2.6 mL, 27.2 mmol) was added dropwise within 5 min at room temperature in air. The reaction mixture was stirred for 1 h then quenched with cold water (100 mL). The resulting mixture was extracted three times with chloroform (30 mL). The combined organic layer was dried over anhydrous magnesium sulfate. The solvent was removed under reduced pressure to produce an orange oil. The crude product was crystallized in dichloromethane and hexanes yielded the product as a grey solid (10.290 g, 62%). ^{1}H NMR ($CDCl_3$, 300 MHz, ppm): δ 7.333 (d, *J* = 0.9 Hz, 1H, aryl - H), 7.104 (d, *J* = 0.9 Hz, 1H, aryl - H), 4.585 (s, 2H, methyl - H), 1.434 (s, 9H, *tert*-butyl - H), 1.297 (s, 9H, *tert*-butyl - H).

2.2.3 Synthesis of $Fc^{ONO}H_2$

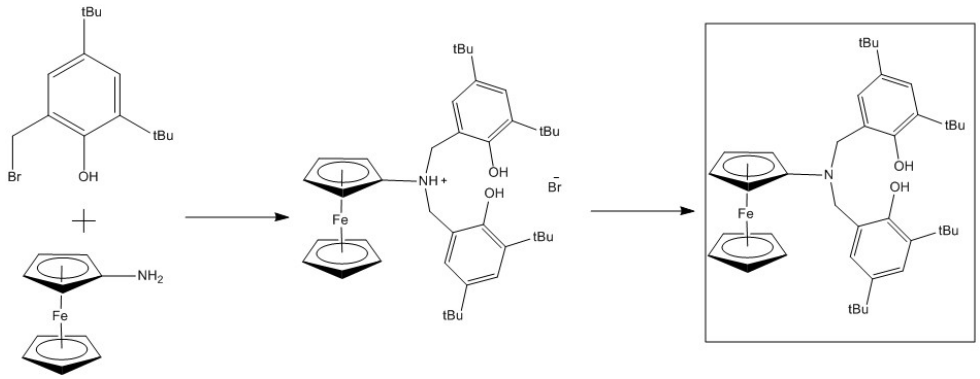

Figure 2-7: Scheme of proligand $Fc^{ONO}H_2$ synthesis.

To a stirring suspension of aminoferrocene (200 mg, 0.995 mmol) and K_2CO_3 (600 mg, 4.34 mmol) in THF (6 mL) a solution of 6-bromomethyl-2,4-di-*tert*-butyl-phenol in THF (4 mL) was added dropwise. After stirred for 12 h additional K_2CO_3 (600 mg, 4.34 mmol) was added to the mixture and the reaction was allowed to stir for another 2 h. The solvent was removed under reduced pressure. The residue was extracted five times with hexanes (3 mL) and filtered over Celite using pipette filter. The solvent of the combined solutions was removed under reduced pressure to produce an orange solid. The crude product was crystallized in hexanes yielded the product as an orange solid (344 mg, 51%). ^{1}H NMR ($CDCl_3$, 300 MHz, ppm): δ 7.330 (s, 2H, phenyl - H), 7.241 (d, J = 1.2 Hz, 2H, aryl - H), 6.836 (d, J = 1.2 Hz, 2H, aryl - H), 4.278 (s, 5H, unsubstituted C - H), 4.074 (s, 4H, methyl - H), 4.029 (t, J = 1.9 Hz, 2H, substituted Cp - H), 3.991 (t, J = 1.9 Hz, 2H, substituted Cp - H), 1.406 (s, 18H, *tert*-butyl - H), 1.278 (s, 18H, *tert*-butyl - H).

2.3 Discussion and Results

There are several published procedures for synthesizing the first precursor of the proligand, aminoferrocene. As early as 1955, Arimoto and Haven developed the first aminoferrocene synthetic pathway with ferrocenecarboxylic acid as the starting material and relatively harsh reaction conditions[66]. This procedure was later modified by other researchers and new protocols using ferrocene as the starting material with milder reaction conditions were also developed and reported[67]. The procedure used in this thesis is modified from the 1,1'-diaminoferrocene synthesis protocol reported by Arnold and coworkers[61]. All the reagents are commonly used in our group and are commercially available.

The procedures for the synthesis of 1,1'-dilithioferrocene and 1,1'-dibromoferrocene were adapted from published reports and similar results were obtained. In the synthesis of bromoferrocene, while repeating the reported procedure, both ferrocene and 1,1'-dibromoferrocene appeared in the crude product. To eliminate the 1,1'-dibromoferrocene impurity, which is difficult to separate from bromoferrocene, 2.5% additional ^{n}BuLi was added to the reaction compared to the reported procedure. Two additional work-up steps were also added to increase the purity of the product. With a similar crude yield as the reported reaction, an aqueous $FeCl_3$ wash was performed to remove the ferrocene impurity that utilized the rapid electron transfer reaction between unsubstituted ferrocene and the iron(III) ion in the solution. Crystallization was done to separate the desired product from trace 1,1'-dibromoferrocene. Although the two additional purification steps result in a lower yield of this reaction, it is difficult to separate ferrocene and 1,1'-dibromoferrocene from the product by column chromatography, which generally grants less product loss.

The reaction time for azidoferrocene synthesis was modified from published reports. The original protocol for 1,1'-diazidoferrocene reported by Arnold and coworkers[61] requires 48 h reaction time. When repeating this procedure, a low yield, ranging from 10% - 30%, was often obtained. Tennyson reported the same reaction with a duration of 24 h and a 69% yield. Therefore, the reaction was monitored by ^{1}H NMR spectroscopy to find an optimal reaction time. The spectra revealed that about 85% of conversion was achieved within 6 h, after which the reaction progresses slowly. With a modified reaction time, a better yield for this step was achieved. The hydrogenation of azidoferrocene that produces aminoferrocene was similar to that of 1,1'-diazidoferrocene[61] and the yield was high. Although a purification is often unnecessary as long as the starting material, azidoferrocene, is of high purity, aminoferrocene can be purified by crystallization in methanol if ferrocene or other impurities are present. Linear crystalline blocks form with about 40% loss of the product.

In an effort of to reproduce the reported reaction for 6-methylhydroxyl-2,4-di-*tert*-butyl-phenol, an incomplete reaction was observed and a mixture of starting material and product was obtained. Therefore, in later reactions, an excess amount of formaldehyde was used. The reaction for 6-bromomethyl-2,4-di-*tert*-butyl-phenol was adapted from published procedures[64] except a different purification method was used. Crystallization was performed instead of column chromatography.

An intermediate compound during the last step of proligand synthesis was observed. Its structure was similar to the desired product and was once mistakenly considered as the

proligand. The intermediate is proposed to be a bromide ammonium salt (Figure 2-7). Its solubility in the reaction solvent, THF, is much lower than that of the starting materials and thus it precipitated from the reaction solution. The precipitation likely covered the K_2CO_3 particles in the mixture and resulted in an insufficient contact of K_2CO_3 and the intermediate. This prevented the further reaction that converts the intermediate into the final product. Although finely grinded K_2CO_3 was used in the reaction, a second addition of K_2CO_3 was required for the reaction to complete. The ^{1}H NMR spectrum of the intermediate agrees with the proposed intermediate structure. With the above modifications, the proposed $Fc^{ONO}H_2$ was successfully synthesized and its structure was confirmed by ^{1}H NMR spectroscopy and X-ray diffraction crystallography.

Chapter 3: Metal Complexes Supported by a Tridentate Ferrocenyl Ligand

3.1 INTRODUCTION

Group 3 metal complexes were intensely studied in the past decades due to their increasing applications as catalysts for a wide range of substrates[68]. As such, yttrium complexes have demonstrated outstanding catalytic properties in various types of reactions. For example, in 1996, Abiko and Wang introduced a yttrium complex that works as a highly efficient catalyst in asymmetric silylcyanation of benzaldehyde[33]. Roesky and coworkers developed a hydroamination/cyclization catalytic cycle using a yttrium amide complex[69] (Figure 3-1). A yttrium anilido hydride complex (Figure 3-2) reported by Leng and coworkers shows high reactivity toward a variety of unsaturated substrates, including imine, azobenzene, carbodiimide, isocyanide, and ketone[70]. Xia and coworkers reported an yttrium alkyl complex as a highly active catalyst for $Me_2NH \cdot BH_3$ dehydrocoupling[71] (Figure 3-3).

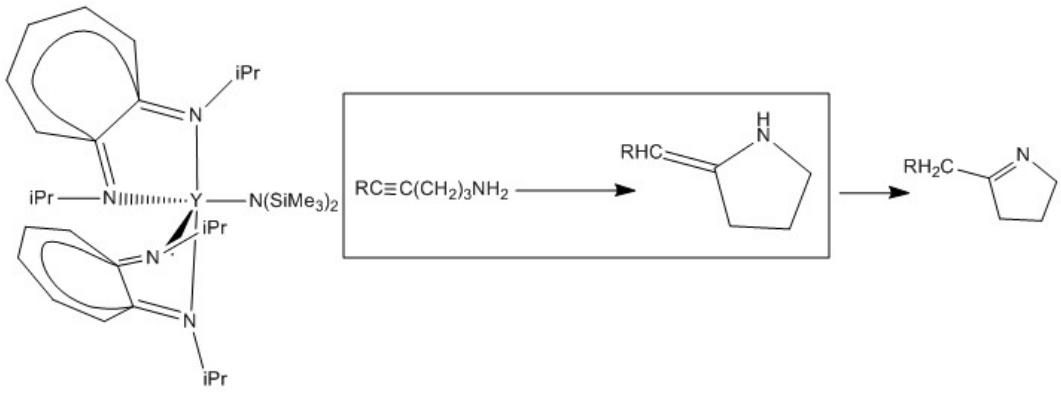

Figure 3-1: A yttrium amide complex in a hydroamination/cyclization catalytic cycle reported by Roesky and coworkers. Reprinted with permission[69].

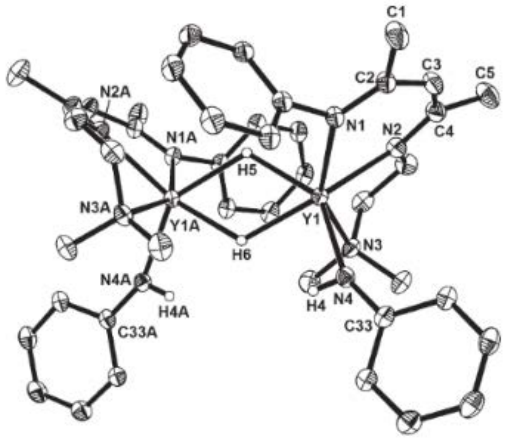

Figure 3-2: Molecular structure of a yttrium anilido hydride complex reported by Leng and coworkers. Thermal ellipsoids are set at the 30% probability level. Isopropyl groups of DIPP, hydrogen atoms (except hydrides and anilide hydrogen atoms), and toluene molecules in the lattice have been omitted for clarity. Reprinted with permission[70].

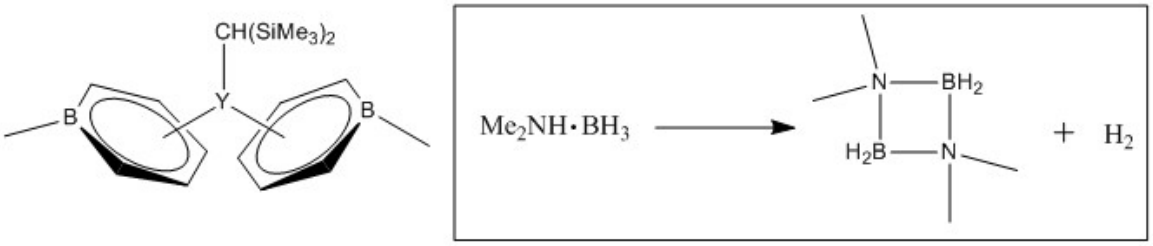

Figure 3-3: Dehydrocoupling of $Me_2NH \cdot BH_3$ catalyzed by a 1-methyl boratabenzene yttrium alkyl complex. Reprinted with permission [71].

Yttrium complexes are also widely investigated catalysts for polymerizations. Numerous studies reported yttrium complexes with high rates of polymerization and high degrees of selectivity. For example, Hessen and coworkers reported a yttrium complex supported by monoanionic tetradentate triamino-amide ligands (Figure 3-4) that was capable of catalyzing ethylene polymerization but with a short catalytic life time[72]. Moingeon and coworkers reported a bis(1,2-azaborolyl) yttrium alkyl complex, which has catalytic activity in methyl methacrylate polymerization with living character[73] (Figure 3-5).

Yttrium complexes are capable initiators not only for the polymerization of simple olefins, but also for ring-opening polymerization reactions of heterocyclic aromatic compounds. Some examples of yttrium catalysts for lactide polymerization reported by Tolman and coworkers[74] and Williams and coworkers[75,76] are shown in Figure 3-6.

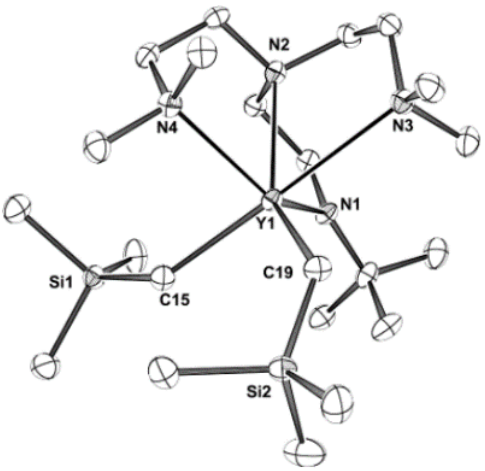

Figure 3-4: Molecular structure of a yttrium complex supported by monoanionic tetradentate triamino-amide ligands reported by Hessen and coworkers. Thermal ellipsoids are drawn at the 50% probability level. Hydrogen atoms have been omitted for clarity. Reprinted with permission from[72].

In an effort to search for efficient catalysts capable of the the polymerization of cyclic esters with a controllable redox-switch, our group synthesized yttrium alkyl complexes supported by a ferrocene-based phosphinimine ligand. Although the cyclic voltammetry study of a yttrium alkyl complexe (NP^{fc})Y(CH_2Ph), which was supported by a bisphosphinimine ferrocene ligand 1,1′-di(2,4-di-*tert*-butyl-6-diphenylphosphinimino phenoxy)ferrocene, indicates a quasi-reversible one-electron redox couple due to the ferrocene-ferrocenium redox pair (Figure 3-7) for possible redox control, this compound

was too unstable to serve as a catalyst[77]. To continue the exploration of redox-switchable yttrium complexes as catalyst candidates, this thesis reports the synthesis of another yttrium complex that is supported by the mono-substituted ferrocene-based tridentate ligand introduced in Chapter 2. Besides its potential catalytic activity, a comparison between this new compound and $(NP^{fc})Y(CH_2Ph)$ may provide a tool for further understanding the influence of iron-yttrium interactions. In addition, yttrium is usually redox inactive, allowing a study of the redox properties associated with a new ligand.

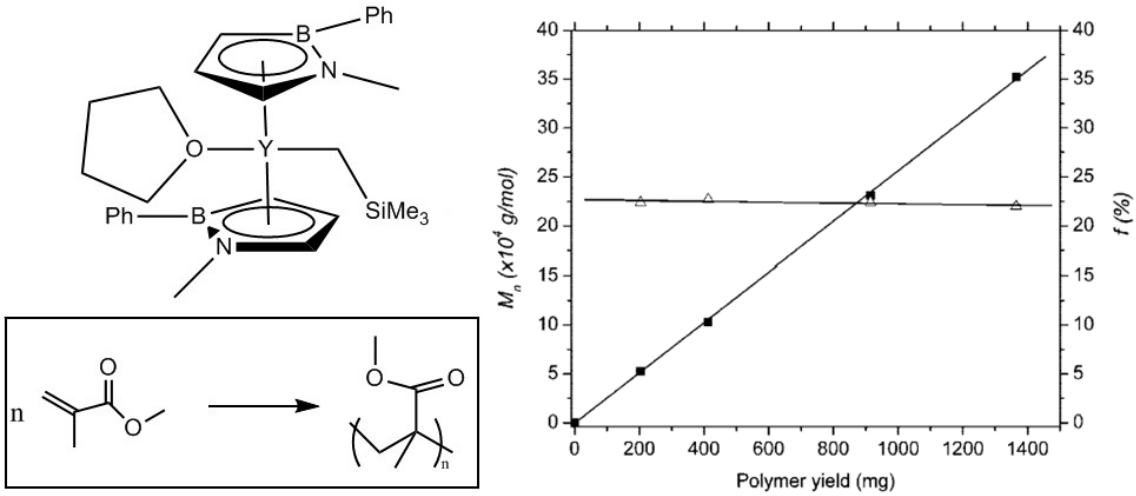

Figure 3-5: Structure of a bis(1,2-azaborolyl) yttrium alkyl complex developed by Moingeon and coworkers that catalyzes living polymerization of methyl methacrylate. Reprinted with permission[73].

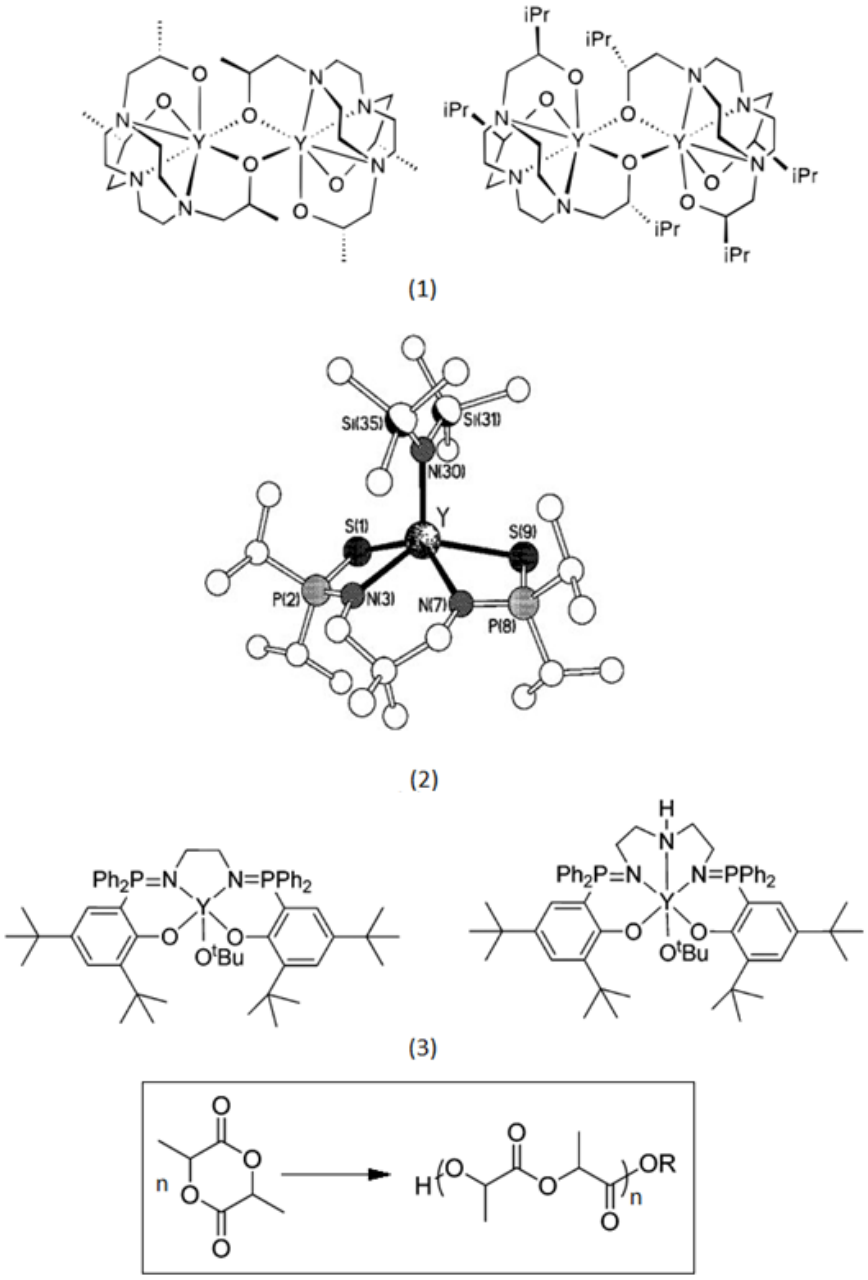

Figure 3-6: Structure of yttrium complexes that initiate lactide polymerization. (1) Dinuclear yttrium complexes reported by Tolman and coworkers. Reprinted with permission[74]. (2) A homoleptic yttrium alkoxide complex reported by Williams and coworkers. Reprinted with permission[76].

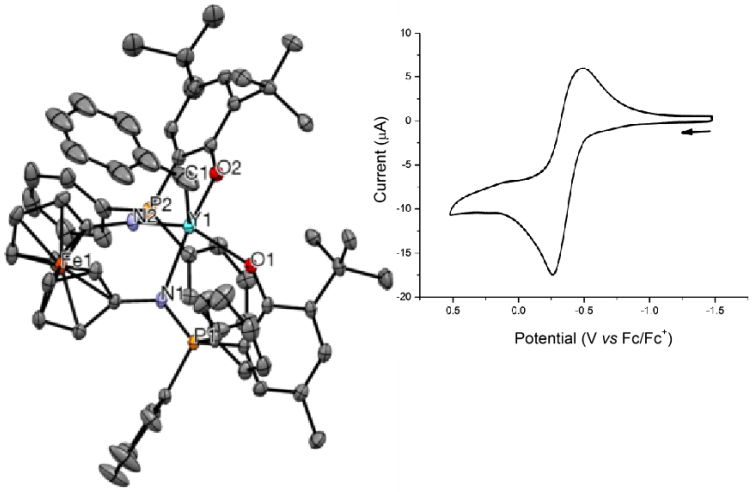

Figure 3-7: Structure of a ferrocene-based phosphinimine yttrium alkyl complex (NP^{fc})Y(CH_2Ph) and its cyclic voltammogram with anodic and cathodic peak potentials of −0.28 and −0.49 V, respectively. Reprinted with permission[73]

.

The lightest group 13 metal, aluminum, which is also usually found in its highest oxidation state in complexes, with the same charge as yttrium, is often used to form adducts with transition metal complexes[43] rather than used in catalysis. However, aluminum complexes demonstrate a unique ability in the ring opening polymerization of lactide[78], with high reactivity and selectivity (Figure 3-8). Considering its potential activity in ring opening polymerization catalysis, the synthesis of an aluminum complex supported by the novel ligand introduced in Chapter 2 is also discussed in this thesis.

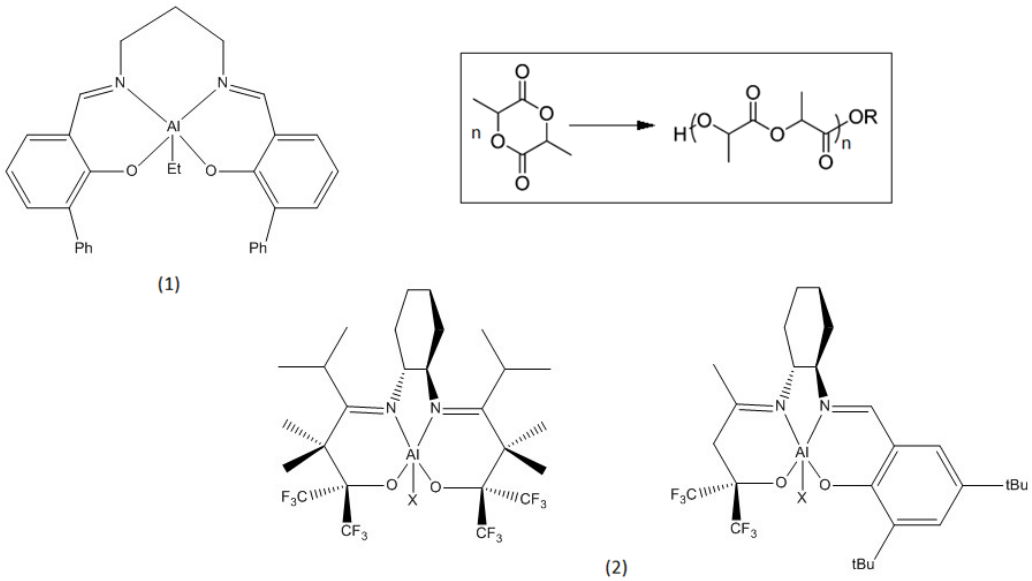

Figure 3-8: Structure of some aluminum complexes with high reactivity and selectivity in lactide ring opening polymerization. (1) Aluminum complexes supported by achiral ligands developed by Aoi and coworkers with chain-end control mechanism. Reprinted with permission[79]. (2) Aluminum complexes supported by fluorinated alkoxide ligands developed by Carpentier and coworkers. X = Me, Cl, OiPr Reprinted with permission[80].

3.2 EXPERIMENTAL

All reactions were performed in an MBraun drybox (less than 1 ppm of O_2/H_2O) unless noted otherwise. All glassware were stored in an oven at 425 K or higher before being brought into the drybox. Solvents were purified using a two-column solid-state purification system by the method of Grubbs[60] and transferred to the drybox without exposure to air. NMR solvents were obtained from Cambridge Isotope Laboratories, degassed, and stored over activated molecular sieves prior to use. NMR spectra were recorded at ambient temperature on Bruker AV-300. Proton chemical shifts are given relative to residual

solvent peaks. All reagents were acquired from commercial sources and used as received unless otherwise noted.

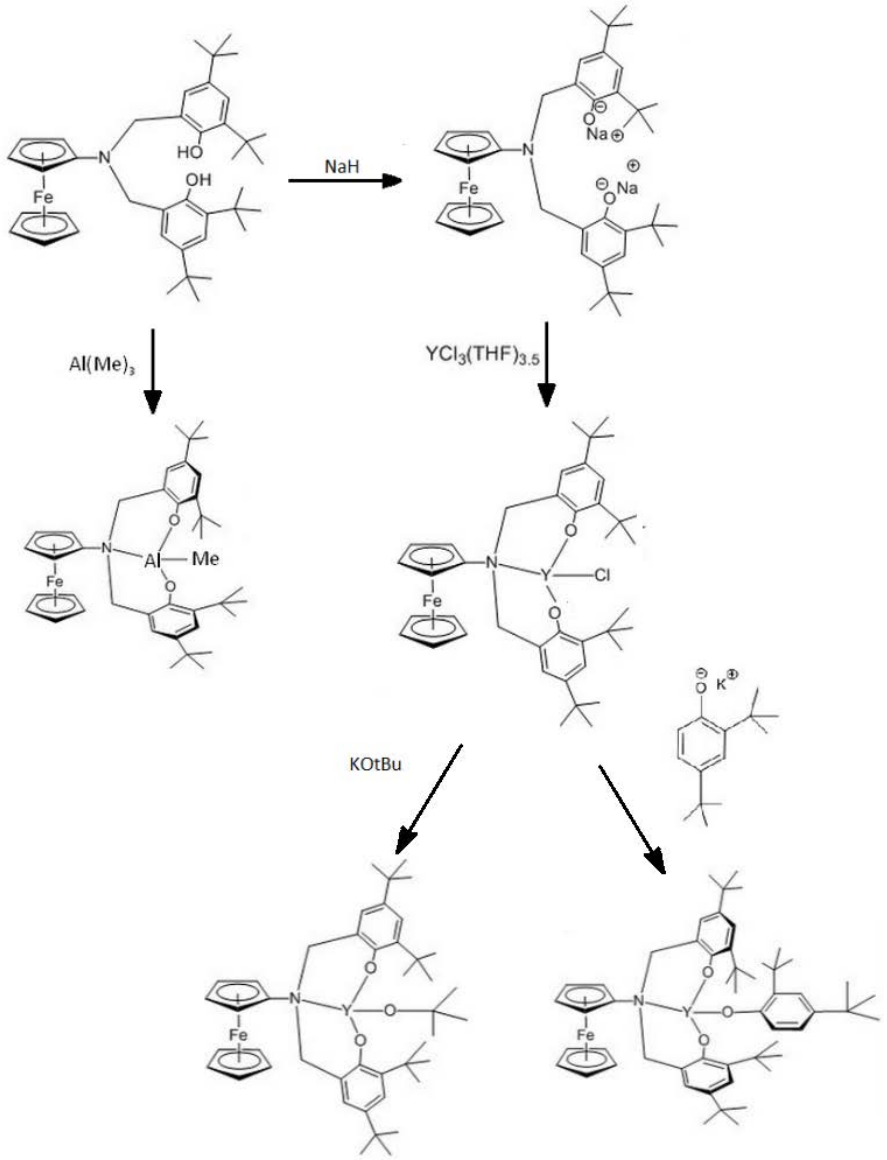

Figure 3-9: Synthetic scheme for yttrium and aluminum complexes supported by a mono-substituted ferrocene ligand.

$Fc^{ONO}Na_2$

To a stirring suspension of NaH (9.4 mg, 0.392 mmol) in THF (3 mL) a solution of Fc^{ONO}-H_2 (50 mg, 0.0784 mmol) in THF (5 mL) was added dropwise at room temperature. The mixture was stirred for 3 h. The resulting mixture was filtered through Celite over pipette filter. The solvent of filtrate was removed under reduced pressure to produce oily yellow solid. The oily solid was rinsed with hexanes (3 mL) yielded product as a yellow solid (47.1 mg, 88%).

$Fc^{ONO}YCl$

To a stirring suspension of $YCl_3 \cdot (THF)_{3.5}$ (56.0 mg, 0.082 mmol) in THF (3 mL) a solution of $Fc^{ONO}Na_2$ in THF (5 mL) was added dropwise at room temperature. The mixture was stirred for 2 h. The solvent of resulting mixture was removed under reduced pressure. The residue was extracted with hexanes and filtered through Celite over pipette filter. The solvent of filtrate was removed under reduced pressure yielded product as a yellow solid (56.301 mg, 90%). ^{1}H NMR (C_6D_6, 300 MHz, ppm): δ 7.562 (s, 2H, aryl - H), 7.192 (s, 2H, aryl - H), 4.281 - 4.247 (overlapped peaks, 9H, 5 unsubstituted Cp - H, 2 substituted Cp - H, 2 methyl - H), 3.781 (s, 2H, broadened methyl - H), 3.651 (s, 2H, substituted Cp - H), 1.657 (s, 18H, *tert*-butyl - H), 1.385 (s, 18H, *tert*-butyl - H).

Attempted synthesis of $Fc^{ONO}Y(O^tBu)$

To a stirring solution of potassium *tert*-butoxide (9.2 mg, 0.823 mmol) in THF (2 mL) a solution of $Fc^{ONO}YCl$ (59.6 mg, 0.0784 mmol) in THF (3 mL) was added dropwise at room temperature. The reaction was stirred for 1 hr. The solvent was removed under reduced

pressure. The residue was not soluble in hexane, diethyl ether, and toluene and was not characterized.

$Fc^{ONO}Y(OPh)$

To a stirring solution of potassium 2,4-di-*tert*-butylphenoxide (56.3 mg, 0.231 mmol) in THF (3 mL) a solution of $Fc^{ONO}YCl$ (166.9 mg, 0.220 mmol) in THF (5 mL) was added dropwise. The reaction was stirred for 1 hr. The solvent was removed under reduced pressure. The residue was extracted with toluene and filtered through Celite over pipette filter. The solvent of filtrate was removed under reduced pressure yielded product as a yellow solid (156.0 mg, 76.4%). ^{1}H NMR (C_6D_6, 300 MHz, ppm): δ 7.644 (d, *J* = 1.5 Hz, 2H, aryl - H,, 7.577 (d, *J* = 1.4 Hz, 2H, aryl - H,, 7.378 - 7.300 (overlapped peaks, 4H, aryl - H,, 4.399 (s, 5H, unsubstituted Cp - H), 4.303 (d, *J* = 7.5 Hz, 2H, methyl - H), 4.0656 (d, *J* = 1.0 Hz, 2H, substituted Cp - H), 3.940 (d, *J* = 7.5 Hz, 2H, methyl - H), 3.354 (d, *J* = 1.0 Hz, 2H, substituted Cp - H), 1.786 (s, 18H, *tert*-butyl - H), 1.761 (s, 9H, *tert*-butyl - H), 1.494 (s, 18H, *tert*-butyl - H), 1.403 (s, 9H, *tert*-butyl - H).

$Fc^{ONO}AlMe$

To a stirring solution of $Al(Me)_3$ (11.3 mg, 0.157 mmol) in hexanes, $Fc^{ONO}H_2$ (100 mg, 0.157 mmol) in hexanes was added dropwise at -78 °C. The mixture was stirred for 1.5 h. Volatile materials were removed under reduced pressure to yield crude product as a yellow solid (95 mg, 89.5%). ^{1}H NMR (C_6D_6, 300 MHz, ppm): δ 7.621 (d, *J* = 1.3 Hz, 2H, aryl - H), 6.887 (d, *J* = 1.3 Hz, 2H, aryl - H), 4.023 (d, *J* = 4.5 Hz, 2H, methyl - H), 3.901 (s, 5H, unsubstituted Cp - H), 3.856 (d, *J* = 4.5 Hz, 2H, methyl - H), 3.779 (d, *J* = 1.1 Hz, 2H,

substituted Cp - H), 3.566 (d, J = 1.1 Hz, 2H, substituted Cp - H), 1.716 (s, 18H, *tert*-butyl - H), 1.410 (s, 18H, *tert*-butyl - H), -0.323 (s, 3H, Al-methyl - H).

3.3 Discussion and Results

The product of $Fc^{ONO}H_2$ deprotonation was not characterized because of its low solubility in both C_6D_6 and $CDCl_3$. However, the ^1H NMR spectra for the succeeding steps agree with the proposed structures of yttrium complexes, implying the success of this reaction. Although $Fc^{ONO}Na_2$ was washed with hexanes to remove residual THF, in most cases, the product was directly carried onto the next step after filtering and without a further work up.

$Fc^{ONO}YCl$ is highly soluble in hexanes, Et_2O, toluene, and THF. When its crystallization was attempted in hexanes and Et_2O, a decomposition product precipitated from the solution. The impurities also remained in the mother liquid without separation from the desired product. When crystallization was attempted in toluene and THF, no precipitation was observed. Decomposition of the yttrium chloride complex was observed within two weeks when stored at -40 °C. Thus, it was made fresh as a starting material for succeeding reactions without further purification.

The exploration of yttrium alkoxide complexes synthesis began with a yttrium *tert*-butoxide compound, $Fc^{ONO}Y(O^tBu)$. Unfortunately, the solubility of this product in various solvents was too low to obtain an NMR spectrum or achieve further purification. Aiming to find a potential candidate as a homogeneous catalyst in polymerization reactions, further

characterization studies on this compound were not conducted. However, a proposed reason for this observation was the formation of a dimeric structure that often leads to low solubility of a compound. In order to break the dimeric structure, a bulky 2,4-di-*tert*-butylphenoxide was introduced into the next yttrium alkoxide complex synthesis.

$Fc^{ONO}Y(OPh)$ was synthesized and characterized; its ^{1}H NMR spectrum agrees with the proposed structure. Crystallization of this compound, however, was unsuccessful which prevented further characterization of this compound including elemental analysis and X-ray diffraction studies. When crystallization was attempted in Et_2O at -40 °C, a mixture of hexanes and Et_2O at -40 °C, and layering of *n*-pentane and benzene at ambient temperature, a powdery precipitate would form. When crystallization was attempted by layering of hexanes and toluene at both -40 °C and ambient temperature, toluene at -40 °C, or layering of hexanes and THF at -40 °C, no precipitate formed. The above attempts were made on a 100 - 150 mg crude product scale. In addition to trying out more solvent combinations, using a larger amount of material are suggested for future crystallization attempts.

$Fc^{ONO}AlMe$ was synthesized and characterized; ; its ^{1}H NMR spectrum agrees with the proposed structure. In comparison with $Fc^{ONO}Y(OPh)$, all peaks of the corresponding protons are shifted downfield in the aluminum complex. This phenomenon is a consequence of the strong Lewis acidity of the metal center. Aluminum effectively draws electron density toward the metal center and causes deshielding of other protons in the complex. Crystallization attempts for further characterization failed for many solvent combinations, including in hexanes, Et_2O, the combination of hexanes and Et_2O, the

combination of hexanes and toluene, and toluene at -40 °C. When the crude product was dissolved in a minimum amount of benzene and a layer of *n*-pentane was carefully added on top of the solution at ambient temperature, an orange crystal formed in two days. Its ^{1}H NMR spectrum suggests that the crystal contains a mixture of more than one compound including the product. Because organoaluminum complexes are usually highly reactive, a proposed explanation is the decomposition of $Fc^{ONO}AlMe$ occurs at room temperature.

Chapter 4: Conclusions

4.1 SUMMARY

A novel mono-substituted ferroceneyl compound, $Fc^{ONO}H_2$, was synthesized. The product was characterized by ^{1}H NMR spectroscopy and X-ray diffraction crystallography. This compound serves as a tridentate proligand, which could support metal complexes with more open coordination spheres around the metal center when compared with the more widely studied tetradentate ferrocenediyl ligands. One expectation from the less hindered metal centers is a higher activity in catalytic processes. Another function of Fc^{ONO} is to provide a platform for investigations of the influence of ferrocene on the catalytic metal center with a reduced direct metal-iron interaction. In addition, this ligand has a potential redox control over the complexes it supports due to the reversible conversion of the iron center in ferrocene between iron(II) and iron(III).

Yttrium alkoxide complexes and an aluminum methyl complex supported by Fc^{ONO} were synthesized. Synthesis of $Fc^{ONO}Y(O^tBu)$ was unsuccessful due to the possible formation of a dimeric structure, as suggested by the low solubility of the product in common solvents. This compound was not further investigated because its lack of solubility limits its application in homogeneous catalytic processes. $Fc^{ONO}Y(OPh)$ and $Fc^{ONO}AlMe$ were synthesized and characterized by ^{1}H NMR spectroscopy. Effective purification procedures were not developed for these two compounds. Attempted crystallization procedures failed to yield single crystals for X-ray diffraction characterization.

4.2 FUTURE DIRECTIONS

Both $Fc^{ONO}Y(OPh)$ and $Fc^{ONO}AlMe$ complexes require further purification and characterization including elemental analysis and X-ray crystallography. Following an effective purification, the redox properties of these complexes should be studied by cyclic voltammetry. The resulting redox behavior should be supported by DFT calculations. Trial experiments of polymerization with a variety of monomers should be conducted using $Fc^{ONO}Y(OPh)$ and $Fc^{ONO}AlMe$ as catalysts in order to explore their catalytic properties and future applications.

Besides additional studies of current compounds, modifications can also be made through changing the alkyl or alkoxide moiety of these complexes. Although the ferrocene scaffold and active metal centers play the most important role in the designed compounds, the monodentate supporting ligand could affect the properties of a metal complex significantly. The yttrium complex supported by ferrocene-based phosphinimine ligand mentioned in Chapter 3 provides a good example[77]. When the alkyl moiety in $(NP^{fc})Y(CH_2Ph)$ was changed to a silyl group, the resulting complex $(NP^{fc})Y(CH_2SiMe_3)$ gave two irreversible oxidation events and an irreversible reduction event by a cyclic voltammetry study, whereas $(NP^{fc})Y(CH_2Ph)$ gave only a quasi-reversible one-electron redox couple (Figure 3-7).

Furthermore, modifications can also be made by altering the metal center. To expand the scope of the current study, other group 3 metals and group 13 metals that have

demonstrated catalytic abilities can be surveyed. Here some scandium complexes and indium complexes and their applications will be briefly reviewed.

Although its size often leads to a decreased catalytic activity of its complexes due to the restricted access to the catalytic site[81,82], scandium, the smallest group 3 metal, is also capable of forming complexes with catalytic activities for polymerization reactions. Cui and coworkers developed a series of heterocyclic-fused cyclopentadienyl scandium bis(alkyl) complexes that catalyze the copolymerization of ethylene and dicyclopentadiene. These highly active catalysts are also regioselective for the two double bonds within dicyclopentadiene[83]. The same group also developed NNN-tridentate pyrrolyl metal complexes of scandium, yttrium, and lutetium. Among those compounds, scandium complexes exhibited high 3,4-selectivity toward the polymerization of isoprene[84]. The structure of these compounds and the reactions they catalyze are shown in Figure 4-1.

There are also examples of scandium complexes as catalysts for the ring opening polymerization of cyclic esters. For example, Lopez-Solera and coworkers synthesized a scandium bis(alkyl) complex (Figure 4-2), which actively initiates the ring opening polymerization of ε-caprolactone with a high conversion and yielded polymers with narrow molecular weight distributions[85].

Our group synthesized scandium alkyl complexes supported by a ferrocene diamide ligand. The ferrocene moiety enforces an open coordination site in a plane perpendicular to the plane bisecting the ferrocene ligand thus allowing the proximity of substrates. The scandium-iron interaction in these complexes were also probed by DFT calculations, which

indicated decreased electrophilicity of the scandium center when the interaction increases. Despite the decomposition of the active species, some of these scandium compounds were capable of catalyzing lactide ring opening polymerization with high conversions[39]. One of the catalytic active scandium complexes is shown in Figure 4-3.

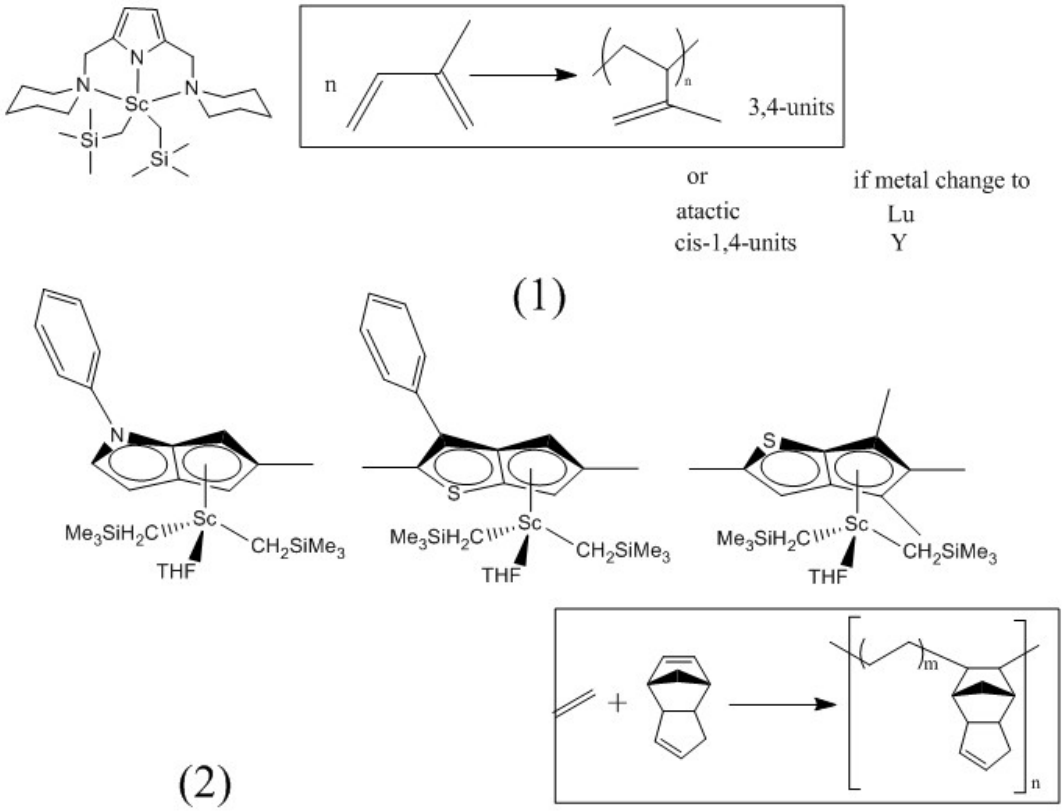

Figure 4-1: Structure of scandium complexes developed by Cui and coworkers and polymerization reactions they catalyze. (1) NNN-tridentate pyrrolyl rare-earth metal complexes that catalyze polymerization of isoprene. Reprinted with permission[84]. (2) Heterocyclic-fused cyclopentadienyl scandium bis(alkyl) complexes that catalyze copolymerization of ethylene and dicyclopentadiene. Reprinted with permission[83].

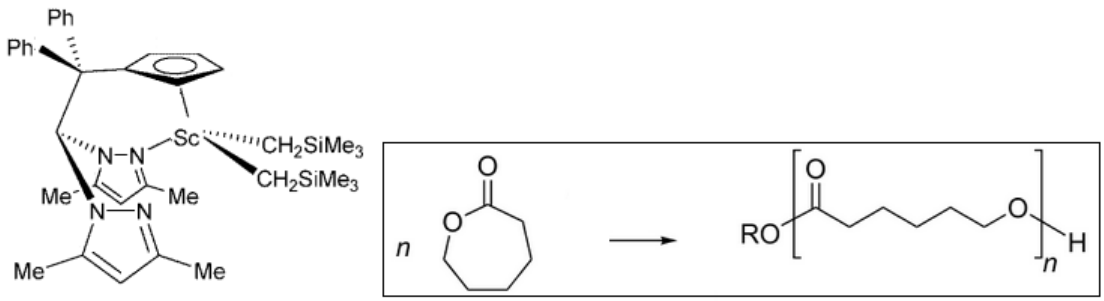

Figure 4-2: Structure of scandium bis(alkyl) complex supported by a NNCp heteroscorpionate ligand developed by Lopez-Solera and coworkers which initiates ring opening polymerization of ε-caprolactone. Reprinted with permission[85].

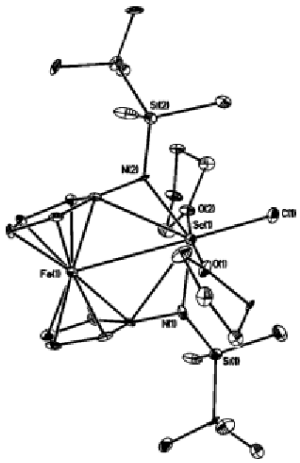

(1)

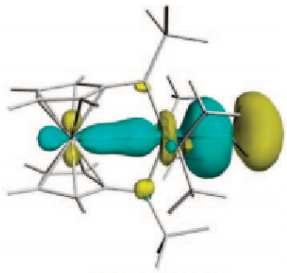

(3)

L-Lactide Polymerization Data for Reactions Catalyzed by 2-Me(THF)$_2$

L-lactide:2-Me(THF)$_2$	M_c	M_n	PDI
100	13 724	52 583	1.33
200	27 448	43 655	1.63
300	41 171	52 151	1.59
400	54 895	69 0828	1.46
500	68 619	80 012	1.52

(2)

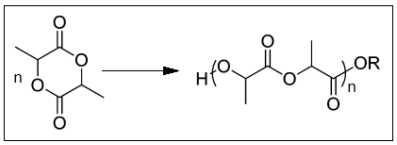

Figure 4-3: Sc(fc[NSi(^{t}Bu)Me$_2$]$_2$)(Me)(THF) complex developed by Diaconescu and coworkers which initiates ring opening polymerization of L-lactide. (1) Structure of the compound with thermal ellipsoid at 35% probability. Hydrogen atoms were omitted for clarity. (2) Tabulated L-lactide polymerization data for reactions catalyzed by Sc(fc[NSi(^{t}Bu)Me$_2$]$_2$)(Me)(THF). (3) Computational models and molecular orbitals that show a scandium-iron interaction for scandium alkyl complexes. Reprinted with permission[39].

Frequently studied along and compared with aluminum complexes[80,86,87], complexes of indium, another group 13 metal, are also investigated for catalytic purposes[88]. Similar to aluminum compounds, investigations on indium complexes are often conducted for their activity in the ring opening polymerization of cyclic esters with high activity[89,90]. Our group synthesized an indium catalyst with the highest reported activity toward CL and BBL polymerization (Figure 1-9) as well as a redox-switchable indium catalyst[51] (Figure 1-12). A kinetic study on aluminum and indium complexes supported by the same ligand for the living ring opening polymerization reaction of lactide conducted by Carpentier and coworkers suggests different operative mechanisms (Figure 4-4); aluminum complexes operate through coordination-insertion, while indium complexes operate through an activated monomer mechanism[87].

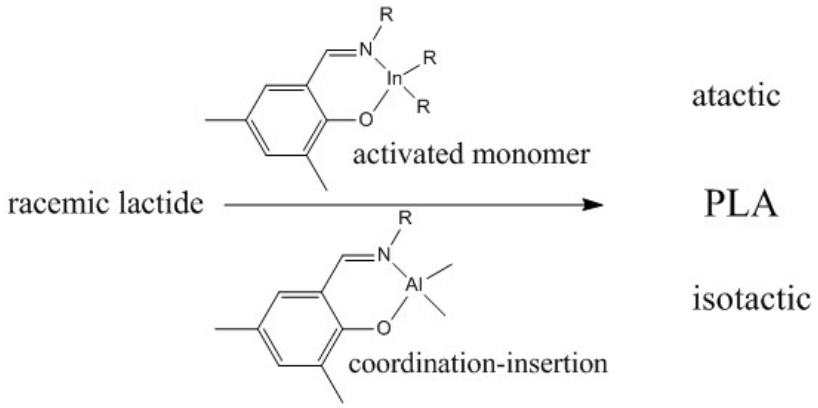

Figure 4-4: Based the stoichiometric reactivity of an aluminum and an indium compounds, two different metal center dependent operative mechanisms for the ring opening polymerization of lactide. Reprinted with permission[87].

These studies encourage the synthesis of scandium and indium complexes supported by the novel ligand introduced in Chapter 2. In fact, the synthesis of an indium complex supported by Fc^{ONO} ligand was attempted at an early stage of this project. Unfortunately, the intermediate product (Figure 2-7) was mistakenly considered as the proligand and was used as starting material. This led to a consequential failure in the indium complex synthesis. Since the proligand synthesis has been correctly achieved, the synthesis of an indium complex should be attempted again. Investigation and comparison of the behaviors of complexes formed by different metals from a same group supported by the same ligand can also expand the understanding of factors influencing their activity in catalysis.

APPENDIX: NMR SPECTRA

1,1'-dibromoferrocene

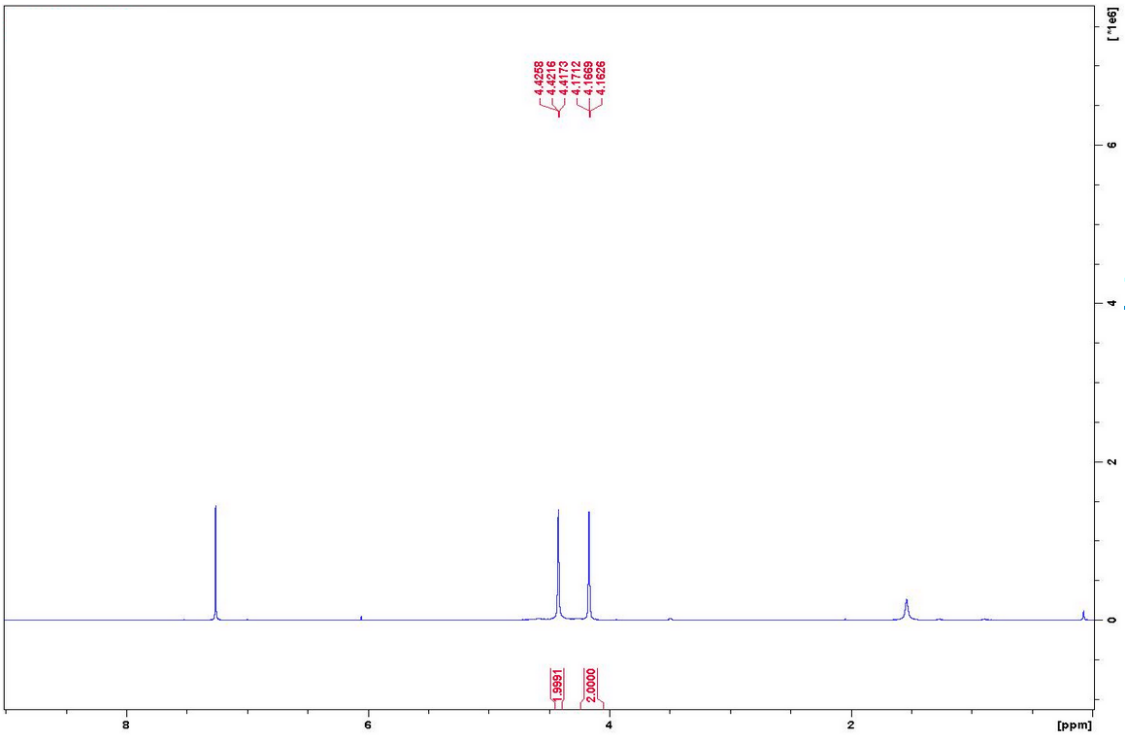

bromoferrocene

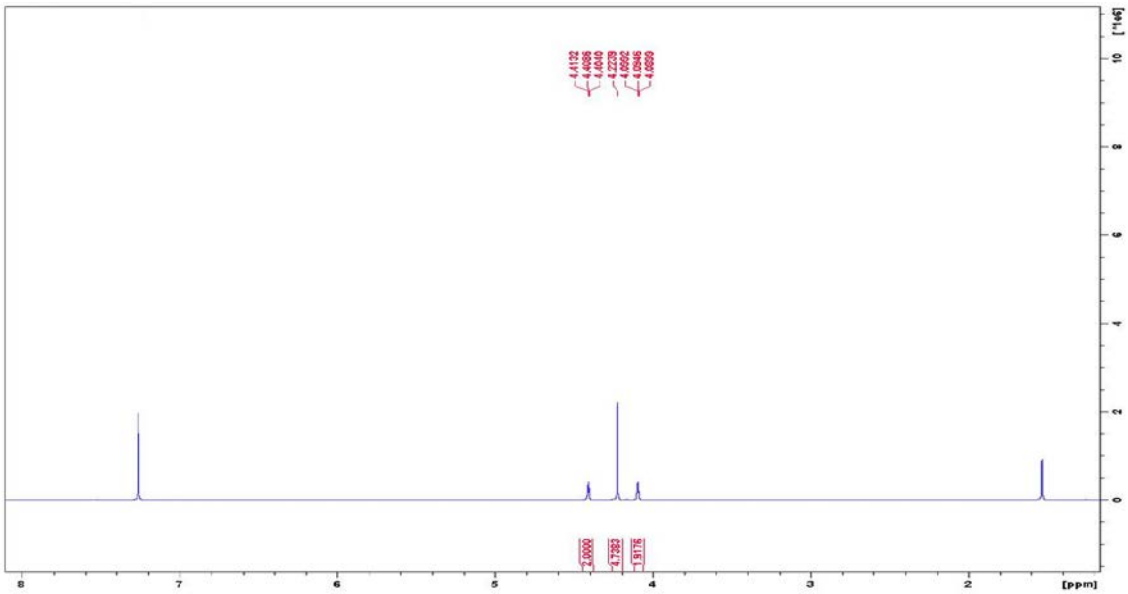

azidoferrocene

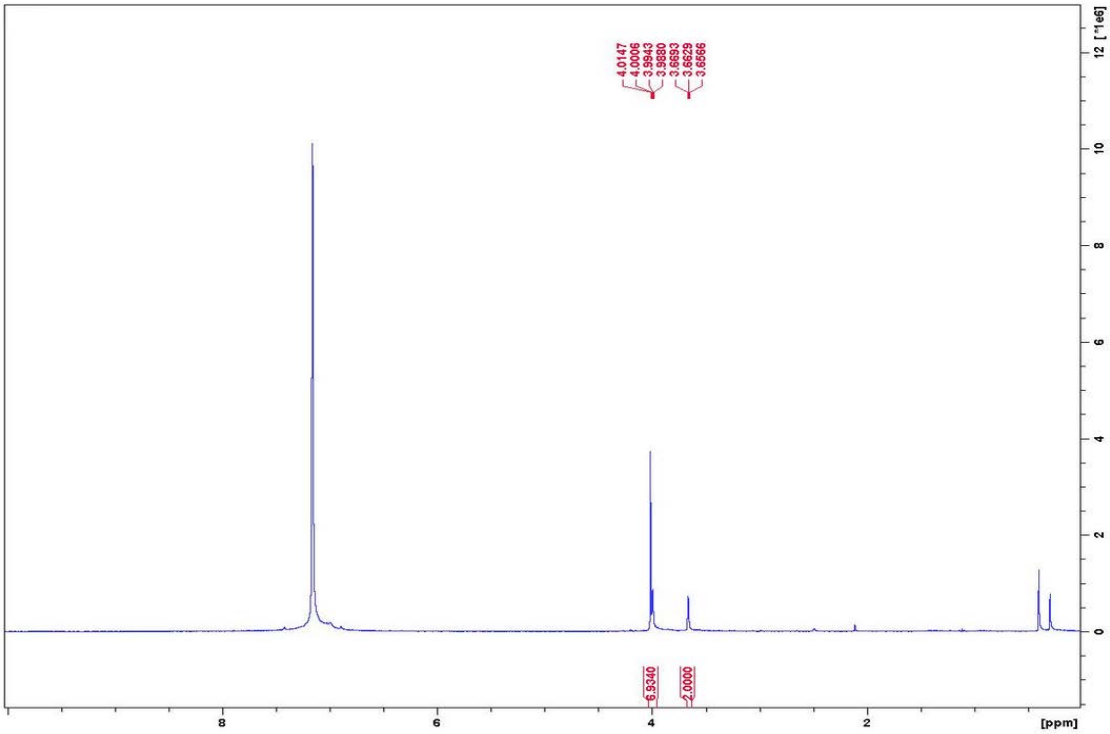

aminoferrocene

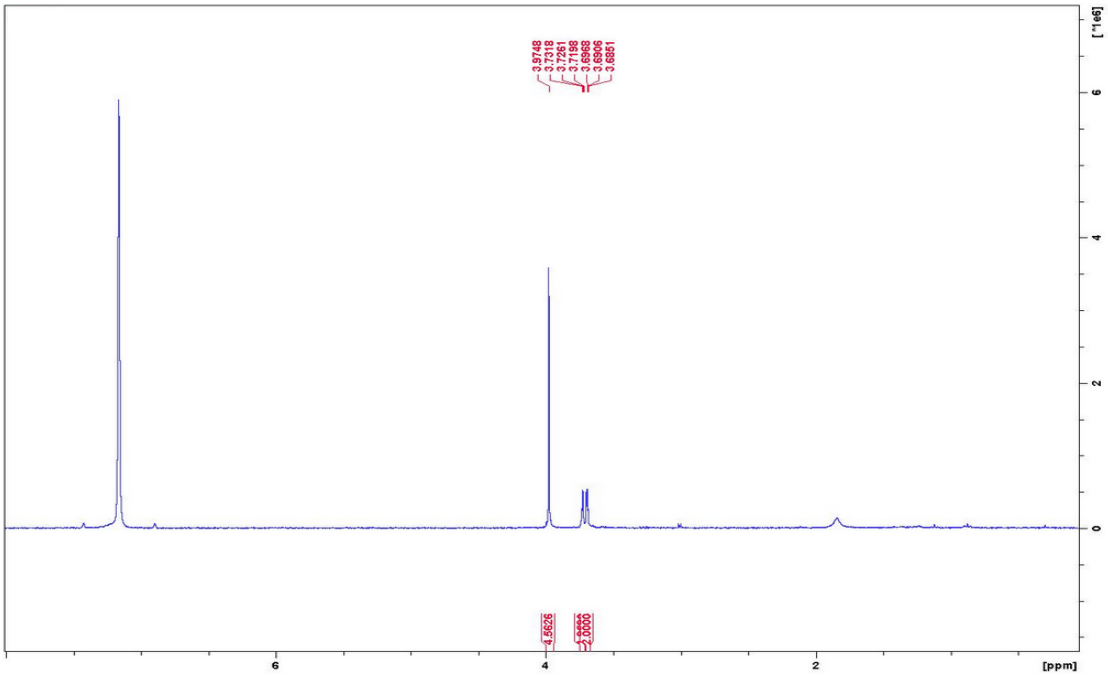

6-methylhydroxyl-2,4-di-*tert*-butyl-phenol

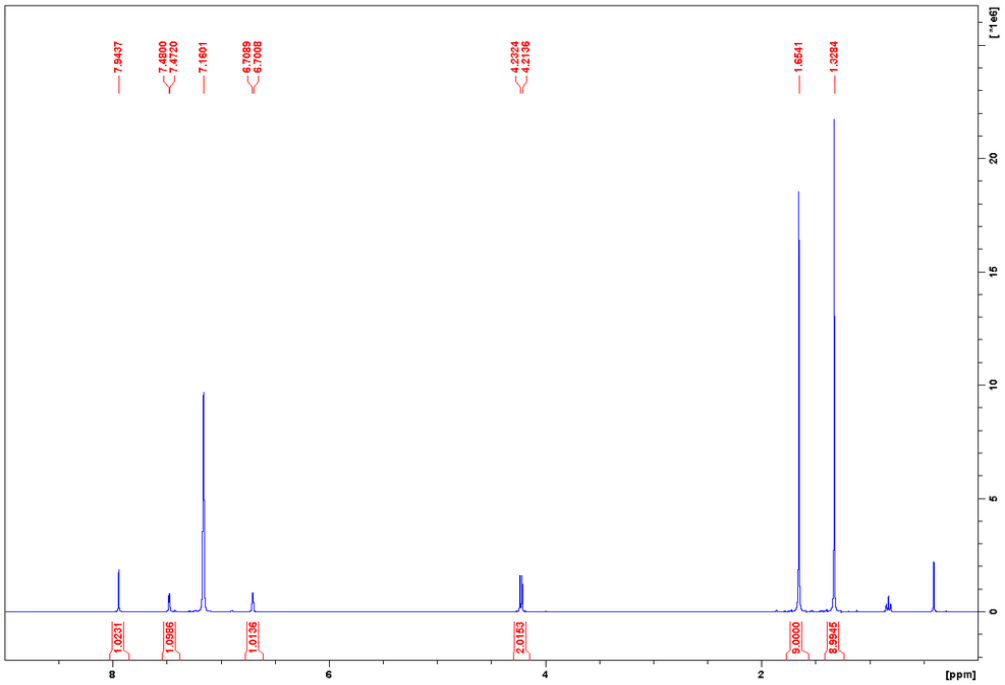

6-bromomethyl-2,4-di-*tert*-butyl-phenol

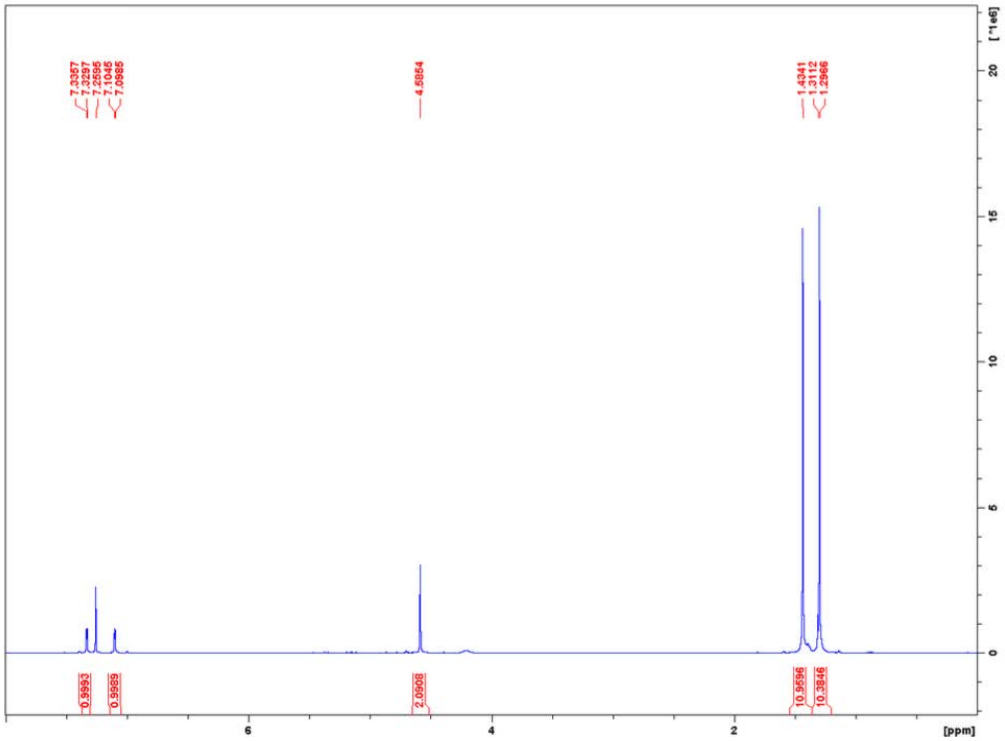

$Fc^{ONO}H_2$

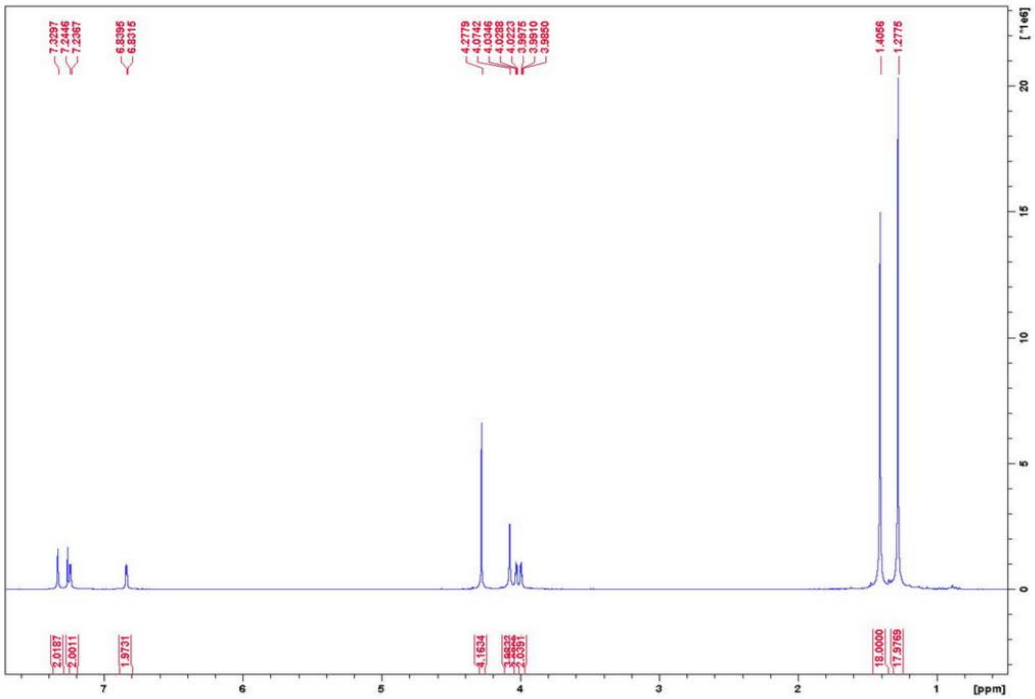

$Fc^{ONO}YCl$

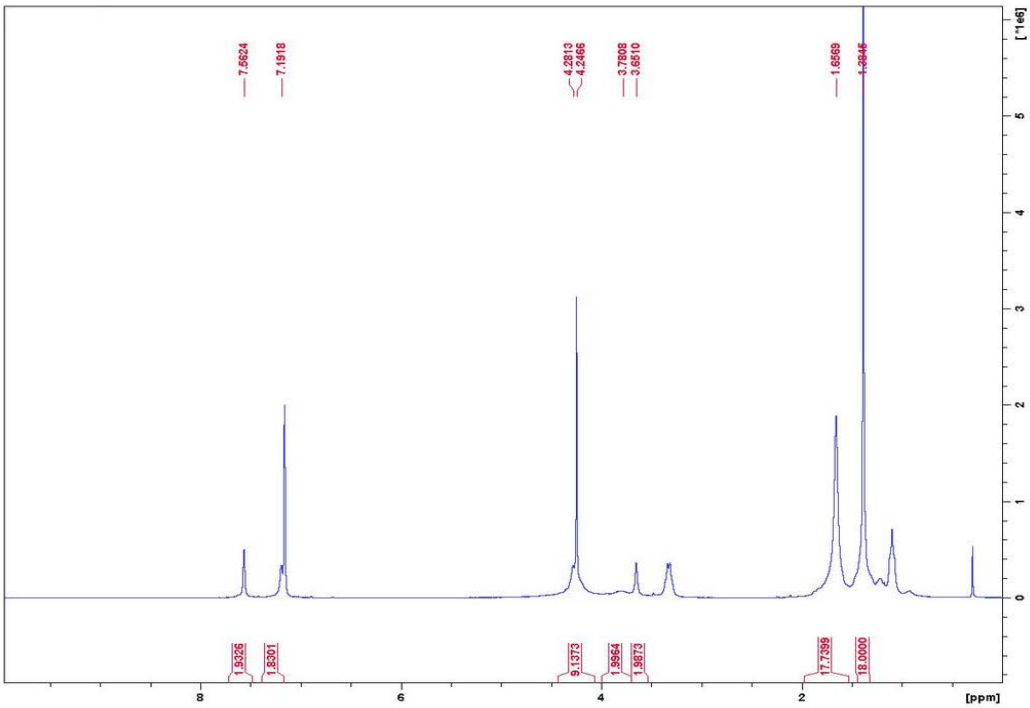

Fc^{ONO}Y(OPh)

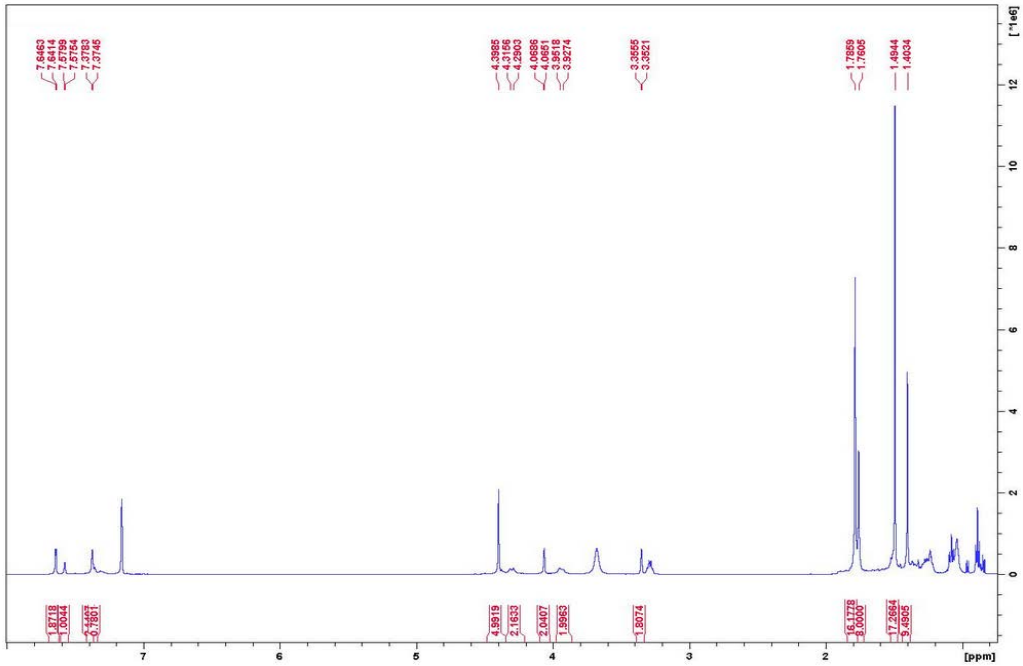

Fc^{ONO}AlMe

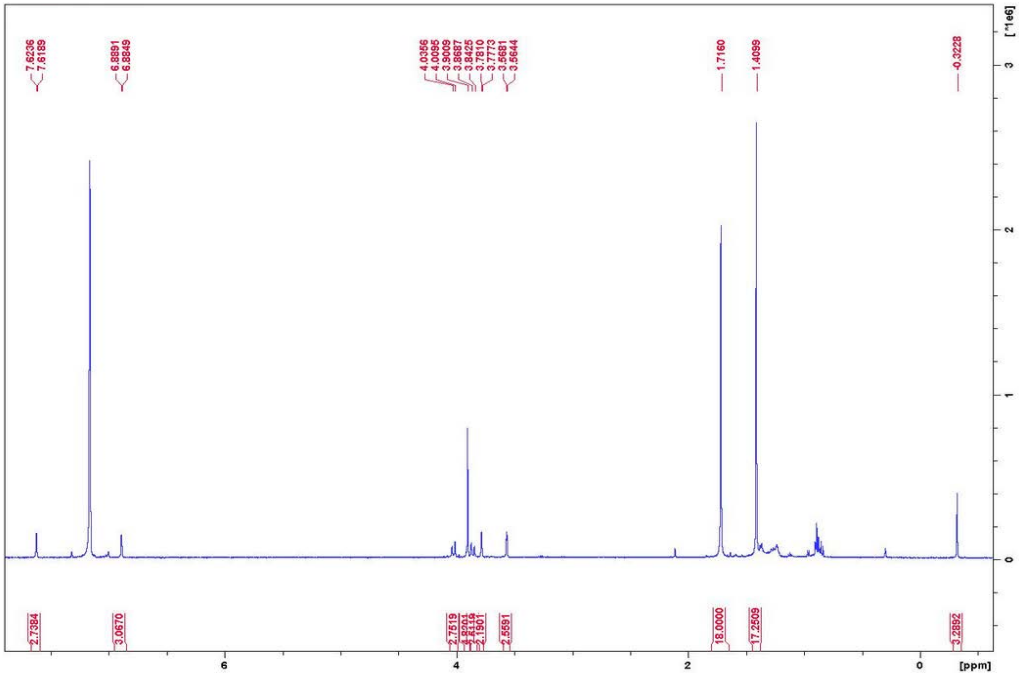

REFERENCES

(1) Crabtree, R. H. *Organometallic Chemistry of the Transition Metals*; John Wiley & Sons, 2011.

(2) Haiduc, I.; Zuckerman, J. J. *Basic Organometallic Chemistry*; Walter de Gruyter, 1985.

(3) Chirik, P. J. *J. Am. Chem. Soc.* **2009**, *131* (10), 3788–3789.

(4) Wilkinson, G.; Rosenblum, M.; Whiting, M. C.; Woodward, R. B. *J. Am. Chem. Soc.* **1985**, *74* (8), 2125–2126.

(5) Rayner-Canham, G.; Overton, T. *Descriptive Inorganic Chemistry, Third Edition*; Macmillan, 2003.

(6) Koepp, H. M.; Wendt, H.; Strehlow, H. Z. *Electrochem.* **1960**, *64*, 483.

(7) Gritzner, G.; Kuta, J. *Pure Appl. Chem.* **1984**, *56*, 461.

(8) Page, J. A.; Wilkingson, G. *J. Am. Chem. Soc.* **1952**, *74* (23), 6149–6150.

(9) Deeming, A. J. *Comprehensive Organometallic Chemistry*; Wilkinson, G., Stone, F. G. A., Abel, E. W., Eds.; Elsevier Science, 1982.

(10) Stepnicka, P. *Ferrocenes: Ligans, Materials and Biomolecules*; John Wiley & Sons, 2008.

(11) Katcho, N. A.; Urones-Garrote, E.; Avila-Brande, D.; Gomez-Herrero, A.; Urbonaite, S.; Csillag, S.; Lomba, E.; Agullo-Rueda, F.; Landa-Canovas, A. R.; Otero-Diaz, L. C. *Chem. Mater.* **2007**, *19* (9), 2304–2309.

(12) Hou, H.; Schaper, A. K.; Weller, F.; Greiner, A. *Chem. Mater.* **2002**, *14*, 3990–3994.

(13) Landis, E. C.; Hamers, R. J. *Chem. Mater.* **2009**, *21*, 724–730.

(14) Lu, M.; He, T.; Tour, J. M. *Chem. Mater.* **2008**, *20* (23), 7352–7355.

(15) Horwitz, C. P.; Dailey, G. C. *Chem. Mater.* **1990**, *2*, 343–346.

(16) Sun, R.; Wang, L.; Yu, H.; Abdin, Z.; Chen, Y.; Huang, J.; Tong, R. *Organometallics* **2014**, *33* (18), 4560–4573.

(17) Wang, X. B.; Dai, B.; Woo, H. K.; Wang, L. S. *Angew. Chem., Int. Ed.* **2005**, *44*, 6022.

(18) Muraoka, T.; Kinbara, K.; Aida, T. *Chem.Commun.* **2007**, 1441.

(19) Iordache, A.; Oltean, M.; Milet, A.; Thomas, F.; Baptiste, B.; Saint-Aman, E.; Bucher, C. *J. Am. Chem. Soc.* **2012**, *134*, 2653–2671.

(20) Blaser, H. U.; Brieden, W.; Pugin, B.; Spindler, F.; Struder, M.; Togni, A. *Top. Catal.* **2002**, *19*, 3–16.

(21) Van Staveren, D. R.; Metzler-Nolte, N. *Chem. Mater.* **2004**, *104* (12), 5931–5986.

(22) Anne, A.; Bouchardon, A.; Moiroux, J. *J. Sm. Chem. Soc.* **2003**, *125*, 1112–1113.

(23) Yu, H.; Shao, L.; Fang, J. *J. Organomet. Chem.* **2007**, *5*, 991–996.

(24) Jeragh, B. J. A.; El-Dissouky, A. *J. Coord. Chem.* **2005**, *12*, 1029–1038.

(25) Fouda, M. F. R.; Abd-Elzaher, M. M.; Abdelsamaia, R. A.; Labib, A. A. *Appl. Organometal. Chem.* **2007**, *21*, 613–625.

(26) Elschenbroich, C. *Organometallics, 3rd ed*; Wiley-VCH, 2006.

(27) Stepnicka, P.; Schneiderova, B.; Schulz, J.; Cisarova, I. *Organometallics* **2013**, *32* (20), 5754–5765.

(28) Chen, J.; Lalancette, R. A.; Jäkle, F. *Organometallics* **2013**, *32* (20), 5843–5851.

(29) Atkinson, R. C. J.; Long, N. J.; Stepnicka, P. *Ferrocenes: Ligans, Materials and Biomolecules*; John Wiley & Sons, 2008.

(30) Buchwalter, P.; Rosé, J.; Braunstein, P. *Chem. Rev.* **2015**, *115* (1), 28–126.

(31) Koridze, A. A.; Kuklin, S. A.; Sheloumov, A. M.; Dolgushin, F. M.; Lagunova, V. Y.; Petukhova, I. I.; Ezernitskaya, M. G.; Peregudov, A. S.; Petrovskii, P. V; Vorontsov, E. V; Baya, M.; Poli, R. *Organometallics* **2004**, *23*, 4585–4593.

(32) Schaarschmidt, D.; Lang, H. *Organometallics* **2013**, *32*, 5668–5704.

(33) Abiko, A.; Wang, G. *J. Org. Chem.* **1996**, *61* (7), 2264–2265.

(34) Ibrahim, A. A.; Wei, P.; Harzmann, G. D.; Kerrigan, N. J. *J. Org. Chem.* **2010**, *75*, 7901–7904.

(35) Gibson, V. C.; Long, N. J.; Oxford, P. J.; White, A. J. P.; Williams, D. J. *Organometallics* **2006**, *25* (8), 1932–1939.

(36) Wang, X.; Thevenon, A.; Brosmer, J. L.; Yu, I.; Khan, S. I.; Mehrkhodavandi, P.; Diaconescu, P. L. *J. Am. Chem. Soc.* **2014**, *136*, 11264–11267.

(37) Duhovic, S.; Oria, J. V; Odoh, S. O.; Schreckenbach, G.; Batista, E. R.; Diaconescu, P. L. *Organometallics* **2013**, *32*, 6012–6021.

(38) Shafir, A.; Arnold, J. *J. Am. Chem. Soc.* **2001**, *123* (37), 9212–9213.

(39) Carver, C. T.; Monreal, M. J.; Diaconescu, P. L. *Organometallics* **2008**, *27* (3), 363.

(40) Monreal, M. J.; Carver, C. T.; Diaconescu, P. L. *Inorg. Chem.* **2007**, *46* (18), 7226.

(41) Gramigna, K. M.; Oria, J. V; Mandell, C. L.; Tiedemann, M. A.; Dougherty, W. G.; Piro, N. A.; Kassel, W. S.; Chan, B. C.; Diaconescu, P. L.; Nataro, C. *Organometallics* **2013**, *32* (20), 5966–5979.

(42) Green, A. G.; Kiesz, M. D.; Oria, J. V; Elliott, A. G.; Buechler, A. K.; Hohenberger, J.; Meyer, K.; Zink, J. I.; Diaconescu, P. L. *Inorg. Chem.* **2013**, *52* (9), 5603–5610.

(43) Bauer, J.; Braunschweig, H.; Dewhurst, R. D. *Chem. Rev.* **2012**, *112* (8), 4329–4346.

(44) Carr, J. D.; Coles, S. J.; Hursthouse, M. B.; Light, M. E.; Munro, E. L.; Tucker, J. H. R.; Westwood, J. *Organometallics* **2000**, *19*, 3312–3315.

(45) Bhadbhade, M. M.; Das, A.; Jeffery, J. C.; McCleverty, J. A.; Badiola, J. A. N.; Ward, M. D. *J. Chem., Soc. Dalt. Trans.* **1995**, 2769.

(46) Sathyaraj, G.; Kiruthika, M.; Weyhermüller, T.; Nair, B. U. *Organometallics* **2012**, *31* (19), 6980–6987.

(47) Ong, J. H. L.; Nataro, C.; Golen, J. A.; Rheingold, A. L. *Organometallics* **2003**, *22* (24), 5027–5032.

(48) Heinze, K.; Reinhardt, S. *Organometallics* **2007**, *26* (22), 5406–5414.

(49) Sussner, M.; Plenio, H. *Angew. Chem., Int. Ed.* **2005**, *44* (18), 6885.

(50) Broderick, E. M.; Guo, N.; Wu, T.; Vogel, C. S.; C. Xu, J. S.; Miller, J. T.; K. Meyer, T. C.; Diaconescu, P. L. *Chem. Commun.* **2011**, *7*, 9897–9899.

(51) Broderick, E. M.; Guo, N.; Vogel, C. S.; Xu, C.; Sutter, J.; Miller, J. T.; Meyer, K.; Mehrkhodavandi, P.; Diaconescu, P. L. *J. Am. Chem. Soc.* **2011**, *133*, 9278–9281.

(52) Diaconescu, P. L. *Comments Inorg. Chem.* **2010**, *31* (5--6), 196–241.

(53) Shafir, A.; Fiedler, D.; Arnold, J. *J. Chem. Soc., Dalt. Trans.* **2002**, 555–560.

(54) Broderick, E. M.; Diaconescu, P. L. *Inorg. Chem.* **2009**, *48* (11), 4701–4706.

(55) Broderick, E. M.; Thuy-Boun, P. S.; Guo, N.; Vogel, C. S.; Sutter, J.; Miller, J. T.; Meyer, K.; Diaconescu, P. L. *Inorg. Chem.* **2011**, *50*, 2870–2877.

(56) Jie, S.; Diaconescu, P. L. *Organometallics* **2010**, *29* (5), 1222–1230.

(57) Duhovic, S.; Diaconescu, P. L. *Polyhedron* **2013**, *52*, 377–388.

(58) Abubekerov, M.; Diaconescu, P. L. *Inorg. Chem.* **2015**, *54*, 1778–1784.

(59) Pettinari, C.; Pettinari 2005 249, 525. *Coord. Chem. Rev.* **2005**, *249*, 525.

(60) Pangborn, A. B.; Giardello, M. A.; Rosen, R. H. G. R. K.; Timmers, F. J. *Organometallics* **1996**, *15* (5), 1518–1520.

(61) Shafir, A.; Power, M. P.; Whitener, G. D.; J. Arnold. *Organometallics* **2000**, *19*, 3978–3982.

(62) Bishop, J. J.; Davison, A.; Katcher, M. L.; Lichtenberg, D. W.; Merrill, R. E.; Smart, J. C. *J. Organomet. Chem.* **1971**, *27*, 241.

(63) Tennyson, A. G.; Khramov, D. M.; Jr., C. D. V.; Creswell, P. T.; Kamplain, J. W.; Lynch, V. M.; Bielawski, C. W. *Organometallics* **2009**, *28*, 5142–5147.

(64) Cepanec, I.; Mikuldaš, H.; Vinkovićb, V. *Syn. Comm.* **2001**, *31* (19), 2913–2919.

(65) Wong, Y.; Mak, C.; Kwan, H.; Lee, H. K. *Inorg. Chima. Acta.* **2001**, *363* (6).

(66) Arimoto, S.; Haven, A. C. J. *J. Am. Chem. Soc.* **1955**, *77*, 6295–6297.

(67) Leonidova, A.; Joshi, T.; Nipkow, D.; Frei, A.; Penner, J.; Konatschnig, S.; Patra, M.; Gasser, G. *Organometallics* **2013**, *32* (6), 2037–2040.

(68) Zimmermann, M.; Anwander, R. *Chem. Rev.* **2010**, *110* (10), 6194–6259.

(69) Burgstein, M. R.; Berberich, H.; Roesky, P. W. *Organometallics* **1998**, *17* (8), 1452–1454.

(70) Lu, E.; Chen, Y.; Leng, X. *Organometallics* **2011**, *30* (20), 5433–5441.

(71) Lu, E.; Yuan, Y.; Chen, Y.; Xia, W. *ACS Catal.* **2013**, *3* (4), 521–524.

(72) Bambirra, S.; Boot, S. J.; Leusen, D.; Meetsma, A.; Hessen, B. *Organometallics* **2004**, *23* (8), 1891–1898.

(73) Fang, X.; Deng, Y.; Xie, Q.; Moingeon, F. *Organometallics* **2008**, *27* (13), 2892–2895.

(74) Chamberlain, B. M.; Sun, Y.; Hagadorn, J. R.; Hemmesch, E. W.; Young, V. G. J.; Pink, M.; Hillmyer, M. A.; Tolman, W. B. *Macromolecules* **1999**, *32*, 2400–2402.

(75) Hodgson, L. M.; White, A. J.; Williams, C. K. *J. Polym. Sci. A Polym. Chem.* **2006**, *44*, 6646–6651.

(76) Bakewell, C.; Cao, T.; Goff, X. F. Le; Long, N. J.; Auffrant, A.; Williams, C. K. *Organometallics* **2013**, *32*, 1475–1483.

(77) Brosmer, J. L.; Diaconescu, P. L. *Organometallics* **2015**, *34*, 2567–2572.

(78) Dechy-Cabaret, O.; Martin-Vaca, B.; Bourissou, D. *Chem. Rev.* **2004**, *104* (12), 6147–6176.

(79) Nomura, N.; Ishii, R.; Akakura, M.; Aoi, K. *J. Am. Chem. Soc.* **2002**, *124* (21), 5938–5939.

(80) Normand, M.; Kirillov, E.; Roisnel, T.; Carpentier, J. F. *Organometallics* **2012**, *31* (4), 1448–1457.

(81) Ge, S.; Meetsma, A.; Hessen, B. *Organometallics* **2009**, *28* (3), 719–726.

(82) Ma, H.; Spaniol, T. P.; Okuda, J. *Angew. Chem.* **2006**, *45*, 7818–7821.

(83) Chen, R.; Yao, C.; Wang, M.; Xie, H.; Wu, C.; Cui, D. *Organometallics* **2015**, *34* (2), 455–461.

(84) Wang, L.; Liu, D.; Cui, D. *Organometallics* **2012**, *31* (17), 6014–6021.

(85) Otero, A.; Fernandez-Baeza, J.; Antinolo, A.; Lara-Sanchez, A.; Martinez-Caballero, E.; Tejeda, J.; Sanchez-Barba, L. F.; Alonso-Moreno, C.; Lopez-Solera, I. *Organometallics* **2008**, *27* (5), 976–983.

(86) Normand, M.; Kirillov, E.; Roisnel, T.; Carpentier, J. F. *Organometallics* **2012**, *31* (15), 5511–5519.

(87) Normand, M.; Dorcet, V.; Kirillov, E.; Carpentier, J. F. *Organometallics* **2013**, *32* (6), 1694–1709.

(88) Gabbai, F. P.; Schier, A.; Riede, J.; Schichl, D. *Organometallics* **1996**, *15* (20), 4119–4121.

(89) Fang, J.; Yu, I.; Mehrkhodavandi, P.; Maron, L. *Organometallics* **2013**, *32*, 6950–6956.

(90) Blake, M. P.; Schwarz, A. D.; Mountford, P. *Organometallics* **2011**, *30* (5), 1202–1214.